tributed to the therapeutic benefit, gained from adding PSL in high-risk patients.

On the other hand, the IVIG + PSL group was at significantly higher risk of relapse despite having a lower risk of overall treatment failure in high-risk patients. In the IVIG + PSL group, 6 of 10 patients relapsed at the steroid tapering phase. Although further examinations are needed to confirm this, we speculate that patients who relapse in the IVIG + PSL group have a severe form of KD, and the relapse is coupled with steroid tapering.

As our simple risk score predicts IVIG unresponsiveness with high sensitivity and specificity, patients in the low-risk group are unlikely to benefit from the addition of corticosteroids. This is important, given that corticosteroids may be associated with many potential adverse reactions.[9–11] Furthermore, epidemiologic and clinical features of KD suggest an infectious etiology,[31] and in general corticosteroid therapy can aggravate infectious processes. This study did not have sufficient statistical power to assess either the likelihood of adverse effects or the effectiveness of therapies in the low-risk group. Therefore, considering the balance between benefit and risk, only KD patients at high risk for nonresponse to IVIG should be given both corticosteroids and IVIG, as part of primary therapy. In addition, a randomized controlled trial suggested the usefulness of corticosteroid therapies in children at the highest risk for resistance to IVIG.[32]

There were several limitations to the study. First, our initial dose of aspirin, which is commonly used in Japan, is lower than that used in the United States. Second, Japanese Ministry of Health criteria used to diagnose CAA might underestimate the true incidence of CAA in patients with KD,[33] though it is a simple set of criteria that are easy to use in clinical settings. Third, this was a retrospective study not a randomized controlled study. A residual confounding effect was not completely ruled out, though we adjusted odds ratios of treatment for sex and for the risk score associated with clinical and coronary outcomes.

In conclusion, IVIG plus PSL might improve coronary and clinical outcomes in patients at high risk of IVIG failure as defined by our simple risk score. Future controlled, randomized clinical trials will define the benefit of this stratification and the role of IVIG + PSL therapy in high-risk KD patients with IVIG failure.

ACKNOWLEDGMENTS

The authors thank all investigators and their staff for their contribution to this study (Shibukawa: Department of Cardiology, Gunma Children's Medical Center; Fukaya: Department of Pediatrics, Fukaya Red Cross Hospital; Takasaki: Department of Pediatrics, Takasaki National Hospital; Tatebayashi: Department of Pediatrics, Tatebayashi Kosei Hospital; Kiryu: Department of Pediatrics, Kiryu Kosei General Hospital; Maebashi: Department of Pediatrics, Gunma Central General Hospital; Maebashi: Department of Pediatrics, Maebashi Red Cross Hospital; Fujioka: Department of Pediatrics, Fujioka General Hospital; Numata: Department of Pediatrics, Tone Central Hospital; Higashiagatuma: Department of Pediatrics, Haramachi Red Cross Hospital; Maebashi: Department of Pediatrics, Saiseikai Maebashi Hospital; and Maebashi: Department of Pediatrics and Developmental Medicine, Gunma University Graduate School of Medicine).

REFERENCES

1. Burns JC, Glode MP. Kawasaki syndrome. *Lancet*. 2004;364:533–544.
2. Suzuki A, Kamiya T, Kuwahara N, et al. Coronary arterial lesions of Kawasaki disease: cardiac catheterization findings of 1100 cases. *Pediatr Cardiol*. 1986;7:3–9.
3. Newburger JW, Takahashi M, Beiser AS, et al. Single intravenous infusion of gamma globulin as compared with four infusions in the treatment of acute Kawasaki syndrome. *N Engl J Med*. 1991;324:1633–1639.
4. Kato H, Koike S, Yokoyama T. Kawasaki disease: effect of treatment on coronary artery involvement. *Pediatrics*. 1979;63:175–179.
5. Shinohara M, Sone K, Tomomasa T, et al. Corticosteroids in the treatment of the acute phase of Kawasaki disease. *J Pediatr*. 1999;135:411–413.
6. Jibiki T, Terai M, Kurosaki T, et al. Efficacy of intravenous immune globulin therapy combined with dexamethasone for the initial treatment of acute Kawasaki disease. *Eur J Pediatr*. 2004;163:229–233.
7. Wooditch AC, Aronoff SC. Effect of initial corticosteroid therapy on coronary artery aneurysm formation in Kawasaki disease: a meta-analysis of 862 children. *Pediatrics*. 2005;116:989–995.
8. Inoue Y, Okada Y, Shinohara M, et al. A multicenter prospective randomized trial of corticosteroids in primary therapy for Kawasaki disease: clinical course and coronary artery outcome. *J Pediatr*. 2006;149:336–341.
9. Miura M, Ohki H, Yoshiba S, et al. Adverse effects of methylprednisolone pulse therapy in refractory Kawasaki disease. *Arch Dis Child*. 2005;90:1096–1097.
10. Takahashi K, Oharaseki T, Wakayama M, et al. Pathological study of ruptured coronary artery aneurysms of Kawasaki disease (KD). In: Abstracts from the 2nd World Congress of Pediatric Cardiology and Cardiac Surgery; May 11–15, 1997; Honolulu, HI. Abstract 202.
11. Shulman ST. Is there a role for corticosteroids in Kawasaki disease? *J Pediatr*. 2003;142:601–603.
12. Burns JC, Capparelli EV, Brown JA, et al. Intravenous gamma-globulin treatment and retreatment in Kawasaki disease. *Pediatr Infect Dis J*. 1998;17:1144–1148.
13. Kobayashi T, Inoue Y, Takeuchi K, et al. Prediction of intravenous immunoglobulin unresponsiveness in patients with Kawasaki disease. *Circulation*. 2006;113:2606–2612.
14. Ayusawa M, Sonobe T, Uemura S, et al. Revision of diagnostic guidelines for Kawasaki disease (the 5th revised edition). *Pediatr Int*. 2005;47:232–234.
15. Harada K. Intravenous gamma-globulin treatment in Kawasaki disease. *Acta Paediatr Jpn*. 1991;33:805–810.
16. Newburger JW, Takahashi M, Gerber MA, et al. Diagnosis, treatment, and long-term management of Kawasaki disease: a statement for health professionals from the Committee on Rheumatic Fever, Endocarditis, and Kawasaki Disease, Council on Cardiovascular Disease in the Young, American Heart Association. *Circulation*. 2004;110:2747–2771.
17. Rowley AH, Eckerley CA, Jack HM, et al. IgA plasma cells in vascular tissue of patients with Kawasaki disease. *J Immunol*. 1997;159:5946–5955.
18. Brown TJ, Crawford SE, Cornwall MI, et al. CD8 T lymphocytes and macrophages infiltrate coronary artery aneurysms in acute Kawasaki disease. *J Infect Dis*. 2001;184:940–943.
19. Wright DA, Newburger JW, Baker A, et al. Treatment of immune globulin-resistant Kawasaki disease with pulsed doses of corticosteroids. *J Pediatr*. 1996;128:146–149.
20. Dale RC, Saleem MA, Daw S, et al. Treatment of severe complicated Kawasaki disease with oral prednisolone and aspirin. *J Pediatr*. 2000;137:723–726.
21. Hashino K, Ishii M, Iemura M, et al. Re-treatment for immune globulin-resistant Kawasaki disease: a comparative study of additional immune globulin and steroid pulse therapy. *Pediatr Int*. 2001;43:211–217.
22. Burns JC, Mason WH, Hauger SB, et al. Infliximab treatment for refractory Kawasaki syndrome. *J Pediatr*. 2005;146:662–667.
23. Raman V, Kim J, Sharkey A, et al. Response of refractory Kawasaki disease to pulse steroid and cyclosporin A therapy. *Pediatr Infect Dis J*. 2001;20:635–637.
24. Imagawa T, Mori M, Miyamae T, et al. Plasma exchange for refractory Kawasaki disease. *Eur J Pediatr*. 2004;163:263–264.
25. Wallace CA, French JW, Kahn SJ, et al. Initial intravenous gamma globulin treatment failure in Kawasaki disease. *Pediatrics*. 2000;105:e78.
26. Durongpisitkul K, Soongswang J, Laohaprasitiporn D, et al. Immunoglobulin failure and retreatment in Kawasaki disease. *Pediatr Cardiol*. 2003;24:145–148.
27. Furukawa S, Matsubara T, Yone K, et al. Kawasaki disease differs from anaphylactoid purpura and measles with regard to tumor necrosis factor-alpha and interleukin 6 in serum. *Eur J Pediatr*. 1992;151:44–47.

28. Inoue Y, Kato M, Kobayashi T, et al. Increased circulating granulocyte colony-stimulating factor in acute Kawasaki disease. *Pediatr Int*. 1999;41: 330–333.

29. Okada Y, Shinohara M, Kobayashi T, et al. Effect of corticosteroids in addition to intravenous gamma globulin therapy on serum cytokine levels in the acute phase of Kawasaki disease in children. *J Pediatr*. 2003;143:363–367.

30. Lin CY, Lin CC, Hwang B, et al. Cytokines predict coronary aneurysm formation in Kawasaki disease patients. *Eur J Pediatr*. 1993;152:309–312.

31. Burns JC, Cayan DR, Tong G, et al. Seasonality and temporal clustering of Kawasaki syndrome. *Epidemiology*. 2005;16:220–225.

32. Newburger JW, Sleeper LA, McCrindle BW, et al. Randomized trial of pulsed corticosteroid therapy for primary treatment of Kawasaki disease. *N Engl J Med*. 2007;356:663–675.

33. de Zorzi A, Colan SD, Gauvreau K, et al. Coronary artery dimensions may be misclassified as normal in Kawasaki disease. *J Pediatr*. 1998; 133:254–258.

THE JOURNAL OF BIOLOGICAL CHEMISTRY VOL. 284, NO. 13, pp. 8548–8556, March 27, 2009

FBP17 Mediates a Common Molecular Step in the Formation of Podosomes and Phagocytic Cups in Macrophages*[S]

Received for publication, July 23, 2008, and in revised form, December 29, 2008 Published, JBC Papers in Press, January 20, 2009, DOI 10.1074/jbc.M805638200

Shigeru Tsuboi[‡1], **Hidetoshi Takada**[§], **Toshiro Hara**[§], **Naoki Mochizuki**[¶], **Tomihisa Funyu**[‖], **Hisao Saitoh**[‖], **Yuriko Terayama**[‖], **Kanemitsu Yamaya**[‖], **Chikara Ohyama**[**], **Shigeaki Nonoyama**[‡‡], **and Hans D. Ochs**[§§]

From the [‡]Infectious and Inflammatory Disease Center, Burnham Institute for Medical Research, La Jolla, California 92037, the [§]Department of Pediatrics, Graduate School of Medical Sciences, Kyushu University, Fukuoka 812-8582, Japan, the [¶]Department of Structural Analysis, National Cardiovascular Center Research Institute, Osaka 565-8565, Japan, the [‖]Oyokyo Kidney Research Institute, Hirosaki 036-8243, Japan, the [**]Department of Urology, Hirosaki University School of Medicine, Hirosaki 036-8562, Japan, the [‡‡]Department of Pediatrics, National Defense Medical College, Saitama 359-0042, Japan, and the [§§]Department of Pediatrics, Research Center for Immunity and Immunotherapy, Seattle Children's Hospital Research Institute, Seattle, Washington 98101

Macrophages act to protect the body against inflammation and infection by engaging in chemotaxis and phagocytosis. In chemotaxis, macrophages use an actin-based membrane structure, the podosome, to migrate to inflamed tissues. In phagocytosis, macrophages form another type of actin-based membrane structure, the phagocytic cup, to ingest foreign materials such as bacteria. The formation of these membrane structures is severely affected in macrophages from patients with Wiskott-Aldrich syndrome (WAS), an X chromosome-linked immunodeficiency disorder. WAS patients lack WAS protein (WASP), suggesting that WASP is required for the formation of podosomes and phagocytic cups. Here we have demonstrated that formin-binding protein 17 (FBP17) recruits WASP, WASP-interacting protein (WIP), and dynamin-2 to the plasma membrane and that this recruitment is necessary for the formation of podosomes and phagocytic cups. The N-terminal EFC (extended FER-CIP4 homology)/F-BAR (FER-CIP4 homology and Bin-amphiphysin-Rvs) domain of FBP17 was previously shown to have membrane binding and deformation activities. Our results suggest that FBP17 facilitates membrane deformation and actin polymerization to occur simultaneously at the same membrane sites, which mediates a common molecular step in the formation of podosomes and phagocytic cups. These results provide a potential mechanism underlying the recurrent infections in WAS patients.

Podosomes (see Fig. 1*A*) are micron-scale, dynamic, actin-based protrusions observed in motile cells such as macrophages, dendritic cells, osteoclasts, certain transformed fibroblasts, and carcinoma cells (1). Podosomes play an important role in macrophage chemotactic migration, which is critical for recruitment of leukocytes to inflamed tissues. Podosomes are both adhesion structures and the sites of extracellular matrix degradation (2). Adhesion to and degradation of the extracellular matrix are essential processes for the successful migration of macrophages in tissues. Podosomes occur in most macrophages and can be observed by differentiating human primary monocytes into macrophages with macrophage-colony stimulating factor-1 (M-CSF-1)[2] and staining the F-actin using phalloidin (3, 4). Podosomes labeled in this way appear as F-actin-rich dots (see Fig. 1*C*). Podosome formation has recently been directly observed *in vitro* and *in vivo* in leukocyte migration through the endothelium, diapedesis (5).

Phagocytosis of bacterial pathogens is one of the most important primary host defense mechanisms against infections. The phagocytic cup (see Fig. 1*B*) is an actin-based membrane structure formed at the plasma membrane of phagocytes, including macrophages, upon stimulation with foreign materials such as bacteria. The phagocytic cup captures and ingests foreign materials, and its formation is an essential first step in phagocytosis leading to the digestion of foreign materials (6, 7). When macrophages are stimulated by foreign materials, podosomes disappear, and phagocytic cups, which are also rich in F-actin, are formed to ingest the foreign materials (see Fig. 1*D*).

Wiskott-Aldrich syndrome (WAS) is an X chromosome-linked immunodeficiency disorder. Patients with WAS suffer from severe bleeding, eczema, recurrent infection, autoimmune diseases, and an increased risk of lymphoreticular malignancy (8–10). The causative gene underlying WAS encodes Wiskott-Aldrich syndrome protein (WASP) (11). WASP deficiency due to the mutation or deletion causes defects in adhesion, chemotaxis, phagocytosis, and the development of hematopoietic cells in WAS patients (10).

* This work was supported, in whole or in part, by National Institutes of Health Grant R01HD042752 (to S. T.). The costs of publication of this article were defrayed in part by the payment of page charges. This article must therefore be hereby marked "*advertisement*" in accordance with 18 U.S.C. Section 1734 solely to indicate this fact.

[S] The on-line version of this article (available at http://www.jbc.org) contains six supplemental figures.

[1] To whom correspondence should be addressed: Dept. of Biochemistry, Oyokyo Kidney Research Institute, 90 Yamazaki, Kozawa, Hirosaki 036-8243, Japan. Tel.: 81-172-87-1221; Fax: 81-172-87-1228; E-mail: tsuboi@oyokyo.jp.

[2] The abbreviations used are: M-CSF-1, macrophage-colony stimulating factor-1; FBP17, formin-binding protein 17; WAS, Wiskott-Aldrich syndrome; WASP, Wiskott-Aldrich syndrome protein; N-WASP, neuronal WASP; WIP, WASP interacting-protein; EFC domain, extended FER-CIP4 homology domain; F-BAR domain, FER-CIP4 homology and Bin-amphiphysin-Rvs domain; PMA, phorbol 12-myristate 13-acetate; GFP, green fluorescence protein; siRNA, short interfering RNA; FITC, fluorescein isothiocyanate; PDZ-GEF, PDZ-guanine nucleotide exchange factor; HEK293 cells, human embryonic kidney 293 cells; HA, hemagglutinin; SH3, src homology 3 domain; dSH3, SH3 domain deletion; GST, glutathione *S*-transferase; , $PI(4,5)P_2$, phosphatidylinositol 4,5-bisphosphate; siFBP, siRNA for FBP17; siC, scrambled control siRNA.

The formation of podosomes and phagocytic cups is severely affected in macrophages from WAS patients (3, 12, 42), suggesting that WASP is involved in the formation of these structures. However, the detailed molecular mechanisms of their formation remain unknown. WASP is complexed with a cellular WASP-interacting partner, WASP-interacting protein (WIP) (13, 14). Recently, two groups (including us) have demonstrated that WASP and WIP form a complex and that the WASP-WIP complex is required for the formation of podosomes (4, 15) and phagocytic cups (16). Here, we identified formin-binding protein 17 (FBP17) as a protein interacting with the WASP-WIP complex and examined the role of FBP17 in the formation of podosomes and phagocytic cups.

EXPERIMENTAL PROCEDURES

Reagents and Antibodies—Recombinant human macrophage-colony stimulating factor-1 (M-CSF-1) was purchased from R&D Systems (Minneapolis, MN). Phenylmethylsulfonyl fluoride, leupeptin, pepstain A, aprotinin, IGEPAL CA-630, paraformaldehyde, saponin, bovine serum albumin, 3-methyladenine, latex beads (3 μm in diameter), phorbol 12-myristate 13-acetate (PMA), human IgG, glycerol, Triton X-100, anti-FLAG monoclonal antibody (M2), and anti-β-actin antibody were purchased from Sigma-Aldrich. The anti-WASP monoclonal antibody, anti-WIP polyclonal antibody, and anti-Myc monoclonal antibody (9E10) were obtained from Santa Cruz Biotechnology Inc. (Santa Cruz, CA). The anti-dynamin-2 antibody was purchased from BD Biosciences. The rat anti-hemagglutinin (HA) monoclonal antibody (3F10) was purchased from Boehringer Ingelheim (Ridgefield, CT). The Cy2-labeled anti-rat IgG was obtained from Jackson ImmunoResearch Laboratories (West Grove, PA).

Yeast Two-hybrid Screening—We screened a human lymphocyte cDNA library (Origene Technology Inc., Rockville, MD) using a full-length WIP as bait. A cDNA encoding full-length WIP was cloned into pGilda (BD Biosciences Clontech). The EGY48 yeast strain was transformed with pGilda-WIP, the human lymphocyte cDNA library, and pSH18–34, a reporter plasmid for the β-galactosidase assay. Transformants were assayed for Leu prototrophy, and a filter assay was performed for β-galactosidase measurement (17).

Cells and Transfection—THP-1 and human embryonic kidney (HEK) 293 cells were purchased from the American Type Culture Collection (Manassas, VA) and cultured in RPMI1640 and Dulbecco's modified Eagle's high glucose medium (Invitrogen), respectively, both supplemented with 10% fetal bovine serum. For human primary monocyte isolation, 10–30 ml of peripheral blood was drawn from healthy volunteers and WAS patients after informed consent was obtained. Monocytes were prepared from peripheral blood samples (10–30 ml) using a monocyte isolation kit II (Miltenyi Biotech Inc., Auburn, CA). Transfection of THP-1 cells and monocytes was performed with a Nucleofector device using a cell line Nucleofector kit V and a human monocyte Nucleofector kit, respectively, according to the manufacturer's instructions (Amaxa Biosystems, Gaithersburg, MD). Transfection of HEK293 cells was performed using SuperFect transfection reagent (Qiagen, Valencia, CA). THP-1 cells and monocytes were co-transfected with the FBP17 constructs and a GFP-expressing plasmid, pmaxGFP (Amaxa Biosystems Inc.), as a transfection marker. The transfection efficiency measured using pmaxGFP was 40–50% for THP-1 cells and 10–20% for monocytes.

RNA Interference—A short interfering RNA (siRNA) for FBP17 and its scrambled control siRNA was synthesized by Dharmacon (Lafayette, CO). The targeting sequence was 5′-CCCACTTCATATGTCGAAGTCTGTT-3′ (18). THP-1 cells and monocytes were transfected with siRNA using a cell line Nucleofector kit V and a human monocyte Nucleofector kit, respectively, and a Nucleofector device. Cells were co-transfected with an fluorescein isothiocyanate (FITC)-conjugated control siRNA, BLOCK-IT (Invitrogen), as a transfection marker. The transfection efficiency measured using BLOCK-IT was 40–50% for THP-1 cells and 10–20% for monocytes.

Immunoprecipitation—For immunoprecipitation of WASP from THP-1 cells, 2×10^7 cells were lysed in buffer A (50 mM Tris-HCl, pH 7.5, 75 mM NaCl, 1% Triton X-100, 1 mM phenylmethylsulfonyl fluoride, 1 μg/ml leupeptin, 1 μg/ml pepstatin A, 1 μg/ml aprotinin). Lysates were centrifuged at 10,000 × *g* at 4 °C for 15 min. The supernatant was incubated with 2 μg/ml anti-WASP monoclonal antibody (Santa Cruz Biotechnology) at 4 °C for 2 h and then incubated with anti-mouse IgG agarose (Sigma). The resin binding the immune complex was washed three times with 0.5 ml of buffer B (50 mM Tris-HCl, pH 7.5, 10% glycerol, 0.1% Triton X-100), and the complex was eluted with 1× Laemmli's SDS-PAGE sample buffer. Eluted proteins were subjected to SDS-PAGE and analyzed by immunoblotting for WASP, WIP, and FBP17.

GST Pull-down Assay—Glutathione *S*-transferase (GST) and a fusion protein of GST and the src homology 3 (SH3) domain of FBP17 (548–609 amino acids) (GST-FSH3) were purified from *Escherichia coli* (XL-1B) extracts using glutathione-Sepharose-4B. HEK293 cells were transfected with the cDNAs of Myc- or FLAG-tagged protein and lysed in buffer A. Lysates from the transfected cells were incubated with the affinity matrices of GST alone or GST-FSH3 at 4 °C for 1 h. After a 1-h incubation, the matrices were washed five times with buffer A, and pull-down samples were analyzed by immunoblotting using anti-Myc or anti-FLAG antibody.

Immunofluorescence Microscopy—THP-1 cells and monocytes grown on coverslips were differentiated into macrophages by incubation with 12.5 ng/ml PMA (Sigma) and 20 ng/ml M-CSF-1 (R&D Systems), respectively, for 72 h. HEK293 cells were transfected with various cDNA constructs and then cultured on coverslips for 48 h. Cells were fixed with 4% (w/v) paraformaldehyde, permeabilized with 0.1% (w/v) saponin, and blocked with 1% (w/v) bovine serum albumin. Cells were stained with primary antibodies and Alexa Fluor 488- or Alexa Fluor 564-labeled secondary antibodies (Invitrogen). Cells were also stained with Alexa Fluor 568-labeled phalloidin (Invitrogen). Cell staining was examined under a fluorescence microscope (Zeiss Axioplan AR) or an MRC 1024 SP laser point scanning confocal microscope (Bio-Rad).

Assays for the Formation of Podosomes and Phagocytic Cups—The formation of podosomes and phagocytic cups was assayed by visualizing these actin-based membrane structures by F-actin staining as described previously (4, 16). Briefly, podosomes

in differentiated THP-1 cells or macrophages were visualized by F-actin staining with Alexa Fluor 568-phalloidin. To form phagocytic cups in differentiated THP-1 cells or macrophages, latex beads (3 μm, Sigma) were opsonized with 0.5 mg/ml human IgG (Sigma), and cells grown on coverslips were incubated with the IgG-opsonized latex beads at 37 °C for 10 min in the presence of 10 mM 3-methyladenine (Sigma) to stabilize the phagocytic cups (16). The phagocytic cups were then also visualized with Alexa Fluor 568-phalloidin. Cells were examined under a fluorescence microscope (Zeiss Axioplan AR).

Assays for Macrophage Migration and Phagocytosis—For the macrophage migration assay, human macrophages (2×10^5 cells) were plated onto chemotaxis membranes with 5-μm pores (Corning, Acton, MA) coated with 0.15% gelatin/phosphate-buffered saline placed within Boyden chamber inserts. M-CSF-1 was used as a chemoattractant and diluted in serum-containing RPMI 1640 medium in lower chambers. After a 4-h incubation, non-migrating cells were removed by gently wiping the upper surface of the filter. The filter was removed from the inserts using a razor blade and mounted onto glass plates, and the number of migrating cells was counted under a fluorescence microscope. For the phagocytosis assay, human macrophages (1×10^6 cells) were seeded on coverslips and incubated with 0.5 ml of RPMI 1640 medium containing IgG-opsonized latex beads (3 μm) at 4 °C for 10 min, allowing the beads to attach to cells. Phagocytosis was initiated by adding 1.5 ml of preheated RPMI 1640 medium, and the cells were incubated with the beads at 37 °C for 30 min. Control plates were incubated at 4 °C to estimate nonspecific binding of latex beads to the cells. After incubation, the cells were vigorously washed with phosphate-buffered saline, and the number of intracellular latex beads was determined by counting beads within cells under a fluorescence microscope. The percentage of phagocytosis was calculated as the total number of cells with at least one bead as a percentage of the total number of cells counted. At least 100 cells were examined.

Cell Fractionation—To prepare the cytoplasmic and membrane fractions, macrophages (1×10^6 cells) were washed with ice-cold phosphate-buffered saline and suspended in 50 mM Tris-HCl buffer, pH 7.5, containing 1 mM EDTA and proteinase inhibitors as described above. The cell suspensions were sonicated four times on ice for 5 s each using a bath-type sonicator followed by ultracentrifugation at 265,000 × *g* at 4 °C for 2 h. The supernatant was used as the cytosolic fraction, and the pellet was resuspended in 50 mM Tris-HCl, pH 7.5, containing 1 mM EDTA and used as the membrane fraction. Anti-Caspase-3 (Santa Cruz Biotechnology) and anti-sodium potassium ATPase antibodies (AbCam, Inc., Cambridge, MA) were used to determine the purity of the cytosolic and membrane fractions, respectively.

Statistics—Statistically significant differences were determined using the Student's *t* test. Differences were considered significant if $p < 0.05$.

RESULTS

FBP17 Binds to the WASP-WIP Complex and Dynamin-2 in Macrophages—To explore the detailed molecular mechanisms of the formation of podosomes and phagocytic cups, we searched for a protein interacting with the WASP-WIP complex. We identified FBP17 as a WIP-binding protein in a yeast two-hybrid screen using the full-length WIP as bait. FBP17 was originally identified as a protein binding to formin, a protein that regulates the actin cytoskeleton (19). FBP17 is a member of the *Schizosaccharomyces pombe* Cdc15 homology (PCH) protein family (20) and contains an N-terminal extended FER-CIP4 homology (EFC) domain (also known as the FER-CIP4 homology and Bin-amphiphysin-Rvs (F-BAR) domain), protein kinase C-related kinase homology region 1 (HR1), and an SH3 domain (Fig. 1*E*). The EFC/F-BAR domain has membrane binding and deformation activities, and FBP17 is involved in endocytosis in transfected COS-7 cells (18, 21, 22).

To confirm that FBP17 directly interacts with WIP or WASP, we performed GST pull-down assays using a fusion protein of GST and the SH3 domain of FBP17 (GST-FBPSH3). Purified GST and the GST-FSH3 fusion protein were subjected to SDS-PAGE (Fig. 1*F*, *lanes 1* and *2*). The HEK293 transfected cells express the Myc- and FLAG-tagged proteins (Fig. 1*F*, *lanes 3–6*). The results from the GST pull-down assays were shown (Fig. 1*F*, *lanes 7–14*). Both WASP and WIP were pulled down by GST-FSH3 (Fig. 1, *lanes 10* and *14*), indicating that the SH3 domain of FBP17 directly interacts with both proteins.

It has previously been shown that FBP17 binds to N-WASP and dynamin in transfected cells (18, 21). We examined whether FBP17 binds to WASP, WIP, and dynamin-2 in macrophages. THP-1 (human monocyte cell line) cells closely resemble monocyte-derived macrophages when differentiated by stimulation with PMA (23) and form podosomes and phagocytic cups that are morphologically and functionally indistinguishable from those in primary macrophages (supplemental Fig. 1) (4, 16, 23). WASP was immunoprecipitated from the lysates of PMA-differentiated THP-1 cells with an anti-WASP monoclonal antibody (Fig. 1*G*, *lanes 2*, *5*, and *8*) followed by immunoblotting using antibodies to FBP17 (21), WASP, and WIP. Both WIP and FBP17 co-immunoprecipitated with WASP (Fig. 1*G*, *lanes 5* and *8*). FBP17 also co-immunoprecipitated with dynamin-2 (Fig. 1*G*, *lanes 14*). These results, taken together with the results in Fig. 1*F*, suggest that FBP17 binds to the WASP-WIP complex and dynamin-2 in macrophages.

We next used immunofluorescence to examine whether FBP17 localizes at podosomes and phagocytic cups because the WASP-WIP complex is an essential component of podosomes (4, 15) and phagocytic cups (16). THP-1 cells transfected with FLAG-tagged FBP17 (FLAG-FBP17) and differentiated by stimulation with PMA were stained with an anti-FLAG monoclonal antibody to visualize FBP17 and with phalloidin to visualize the F-actin in podosomes and phagocytic cups (Fig. 1, *H* and *I*, *left* and *middle panels*). Merged images revealed that both F-actin and FBP17 are present in podosomes and phagocytic cups (Fig. 1, *H* and *I*, *right panels*), indicating that FBP17 localizes at podosomes and phagocytic cups.

Importance of FBP17 in the Formation of Podosomes and Phagocytic Cups—To determine the importance of FBP17 in the formation of podosomes and phagocytic cups, we knocked down FBP17 in THP-1 cells with siRNAs. To confirm that the expression of FBP17 was knocked down in cells, we transfected THP-1 cells with siRNAs, prepared lysates from the total

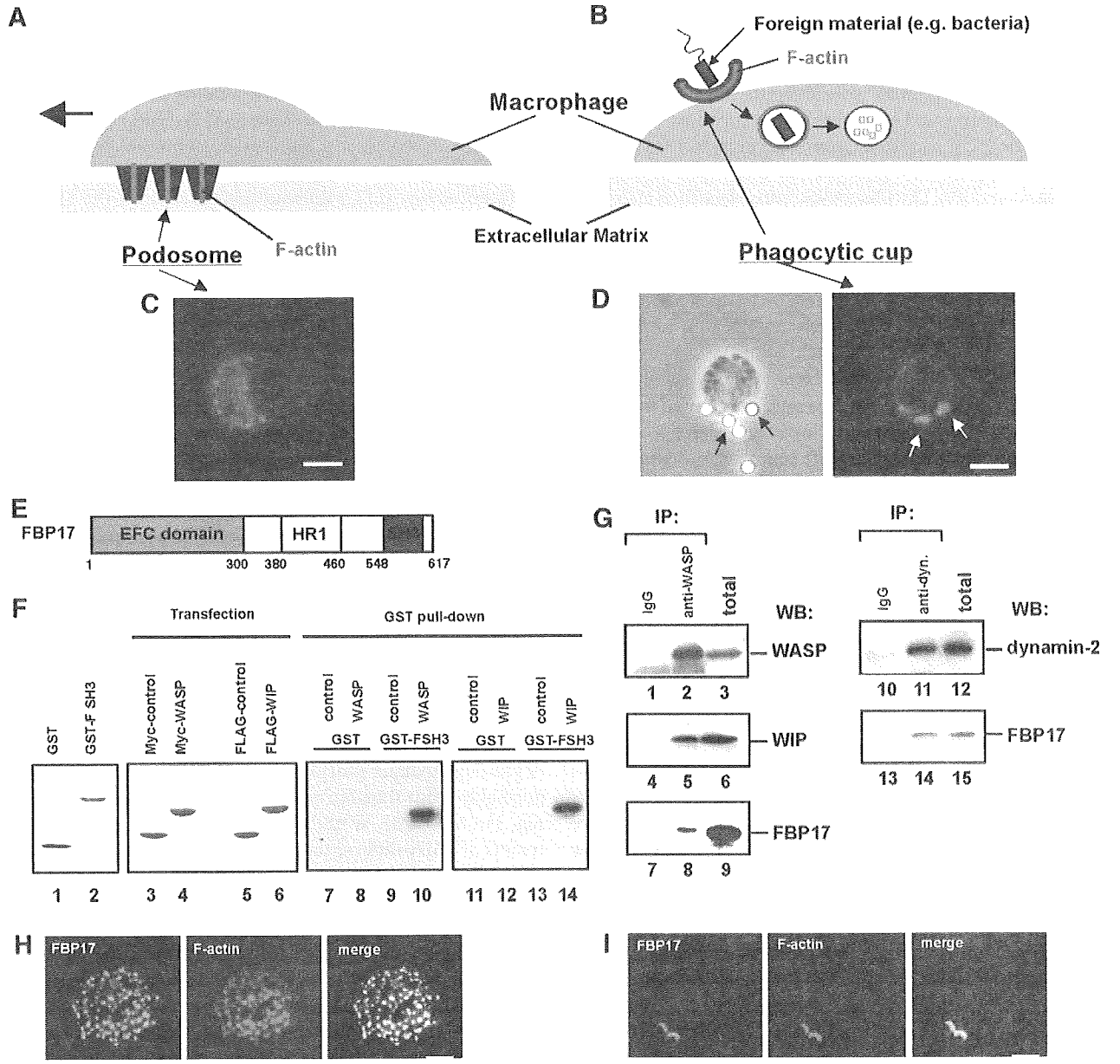

FIGURE 1. **FBP17 is a component of podosomes and phagocytic cups.** *A* and *B*, schematic drawings of podosomes (*A*) and a phagocytic cup (*B*) in macrophages. *C*, podosomes in macrophages were visualized by F-actin staining using Alexa Fluor 568-phalloidin. *D*, macrophages incubated with IgG-opsonized latex beads formed phagocytic cups to ingest the beads. A phase contrast image of a macrophage forming phagocytic cups (*left panel*). *Black arrows* indicate the latex beads ingested by the macrophage. Phagocytic cups were visualized by F-actin staining using Alexa Fluor 568-phalloidin (*right panel*). *White arrows* indicate the phagocytic cups. The *bar* is 10 μm. *E*, the domain organization of FBP17. *HR1*, protein kinase C-related kinase homology region 1. *F*, FBP17 interacts directly with WASP and WIP via its SH3 domain. GST and the GST-FBP17 SH3 domain fusion protein (GST-FSH3) were purified from bacteria extracts. Purified proteins were subjected to SDS-PAGE and stained with Coomassie Brilliant Blue (*lanes 1* and *2*). HEK293 cells were transfected with the cDNAs of Myc-tagged control protein (Myc-PDZ-GEF), Myc-WASP, FLAG-PDZ-GEF, or FLAG-WIP, and the expression of those proteins were analyzed by immunoblotting (*lanes 3–6*). Lysates from the HEK293 transfected cells were incubated with the affinity matrices of GST alone or GST-FSH3. Pull-down samples were analyzed by immunoblotting using anti-Myc antibody (*lanes 7–10*) and anti-FLAG antibody (*lanes 11–14*). *G*, FBP17 binds WASP, WIP, and dynamin-2. WASP was immunoprecipitated (*IP*) from the lysates of PMA-differentiated THP-1 cells with anti-WASP or a control IgG (*left panel, lanes 1–9*). The WASP immunoprecipitates and total lysates were analyzed by immunoblotting (*WB*) for WASP (*lanes 1–3*), WIP (*lanes 4–6*), and FBP17 (*lanes 7–9*). Dynamin was also immunoprecipitated from the THP-1 cell lysates with an anti-dynamin polyclonal antibody. The dynamin immunoprecipitates and total lysates were analyzed by immunoblotting for dynamin-2 (*lanes 10–12*) and FBP17 (*lanes 13–15*). *H* and *I*, confocal laser scanning micrographs of PMA-differentiated THP-1 cells. *H*, THP-1 cells transfected with FLAG-tagged FBP17 cDNA (FBP17) were double-stained with an anti-FLAG monoclonal antibody (*left panel*) and phalloidin (*center panel*) to visualize the F-actin in podosomes. *Yellow* indicates co-localization of FBP17 (*green*) and F-actin, podosomes (*red*) (*right panel*). *I*, THP-1 cells transfected with FLAG-FBP17 cDNA were incubated with IgG-opsonized latex beads and double-stained with anti-FLAG antibody and phalloidin. Phagocytic cups were visualized by F-actin staining (*center panel*). *Yellow* indicates co-localization of FBP17 (*green*) and F-actin, phagocytic cups (*red*) (*right panel*). The *bar* is 10 μm.

siRNAs-transfected cells, and analyzed the expression level of FBP17 by immunoblotting. THP-1 cells transfected with the siRNA for FBP17 expressed ~40% less FBP17 than cells transfected with a scrambled control siRNA based on the immunoblots (Fig. 2*A*, *lanes 1* and *2*) but expressed the same level of β-actin (Fig. 2*A*, *lanes 3* and *4*). The transfection efficiency of

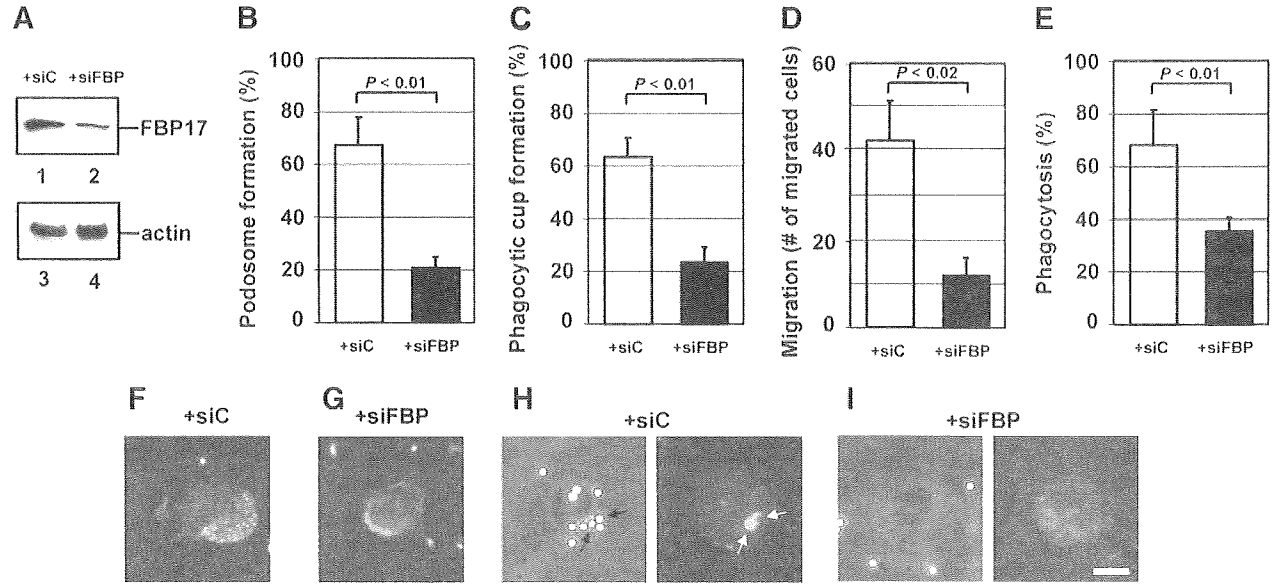

FIGURE 2. **The importance of FBP17 in the formation of podosomes and phagocytic cups.** *A*, expression of FBP17 was reduced by transfection of siRNA. THP-1 cells were transfected with siRNA for FBP17 (siFBP; *lanes 2* and *4*) or its scrambled control siRNA (siC; *lanes 1* and *3*). Lysates prepared from total transfected cells were analyzed by immunoblotting for FBP17 (*lanes 1* and *2*) and β-actin (*lanes 3* and *4*). *B* and *C*, effects of FBP17 siRNA on the formation of podosomes and phagocytic cups in macrophages. Human primary monocytes were co-transfected with siFBP (*closed bars*) or siC (*open bars*) and an FITC-conjugated control siRNA and then differentiated into macrophages with M-CSF-1. FITC-positive transfected cells were examined for the formation of podosomes (*B*) or phagocytic cups (*C*), and the percentage of cells with podosomes or phagocytic cups was scored. *D* and *E*, effects of FBP17 siRNA on the functions of podosomes and phagocytic cups. Macrophages co-transfected with siFBP (*closed bars*) or siC (*open bars*) and the FITC-conjugated control siRNA were assayed for macrophage migration (*D*) or phagocytosis of IgG-opsonized latex beads (*E*). Data represent the mean ± S.D. of triplicate experiments. *F–I*, immunofluorescence micrographs of a representative cell from each experiment. Cells transfected with siC (*F*) and siFBP (*G*) were stained with Alexa Fluor 568-phalloidin. Cells transfected with siC (*H*) or siFBP (*I*) were incubated with IgG-opsonized latex beads and then stained with phalloidin. The *left* and *right panels* are phase contrast and immunofluorescence micrographs, respectively. The *bar* is 10 μm.

THP-1 cells was estimated to be 40–50% from the expression of green fluorescent protein (GFP) used as a transfection control. Therefore, the decrease in FBP17 expression indicates that FBP17 was efficiently knocked down in most transfected cells.

Human primary monocytes were co-transfected with the FBP17 siRNAs and a FITC-conjugated control siRNA as a transfection marker. After differentiation of the monocytes into macrophages with M-CSF-1, FITC-positive cells were examined for the formation of podosomes and phagocytic cups. To quantify their formation, we scored the percentage of cells with podosomes or phagocytic cups among FITC-positive cells. When the expression of FBP17 was knocked down, the formation of both podosomes and phagocytic cups in macrophages was significantly reduced ($p < 0.01$; Fig. 2, *B* and *C*). These results suggest that FBP17 is necessary for the formation of podosomes and phagocytic cups. A representative cell from each experiment is shown in Fig. 2, *F* and *G*, for podosomes and in Fig. 2, *H* and *I*, for phagocytic cups. We then assayed macrophage migration as a podosome function and phagocytosis as a phagocytic cup function. When expression of FBP17 was knocked down, macrophage migration through a gelatin filter toward a chemoattractant was significantly reduced in cells transfected with FBP17 siRNA ($p < 0.02$; Fig. 2*D*). Phagocytosis of IgG-opsonized latex beads was also reduced (Fig. 2*E*). These results suggest that FBP17 is essential for chemotaxis and phagocytosis because of its role in forming podosomes and phagocytic cups, respectively.

FBP17 Recruits the WASP-WIP Complex to the Plasma Membrane—Recent biochemical analyses revealed that FBP17 binds to a membrane phospholipid, phosphatidylinositol 4,5-bisphosphate ($PI(4,5)P_2$), through its EFC/F-BAR domain and to N-WASP and dynamin via its SH3 domain (18, 21, 24). We have shown that although WASP and WIP are cytosolic proteins, the WASP-WIP complex localizes at podosomes and phagocytic cups (4, 16). We then examined whether FBP17 recruits the WASP-WIP complex to the plasma membrane in macrophages. We focused on the roles of the EFC and SH3 domains of FBP17 and constructed three FBP17 mutants for the recruitment experiments: a Lys-33 to Glu (K33E) substitution, a Lys-166 to Ala (K166A) substitution, and an SH3 domain deletion (dSH3). Both substitution mutations in the EFC domain (K33E and K166A) significantly reduce membrane binding and deformation (22), and the dSH3 mutant does not bind to WASP and WIP because the SH3 domain is the binding site of WASP and WIP (Fig. 1*F*). We co-transfected HEK293 cells with the FLAG-tagged FBP17 constructs, WASP, and WIP. A C-terminal fragment (1146–1429 amino acids) of PDZ-GDP exchange factor (PDZ-GEF) was used as a negative control for FBP17 because this fragment is stable in the cytosol and does not interact with any WASP-related proteins (4, 16, 25). We confirmed the expression of FBP17 and its mutants in cells by immunoblotting (supplemental Fig. 2) and immunoprecipitated FLAG-tagged proteins from lysates of the transfected cells with anti-FLAG antibody (Fig. 3*A*, *lanes 1–5*). WASP and WIP were detected in the immunoprecipitates from cells

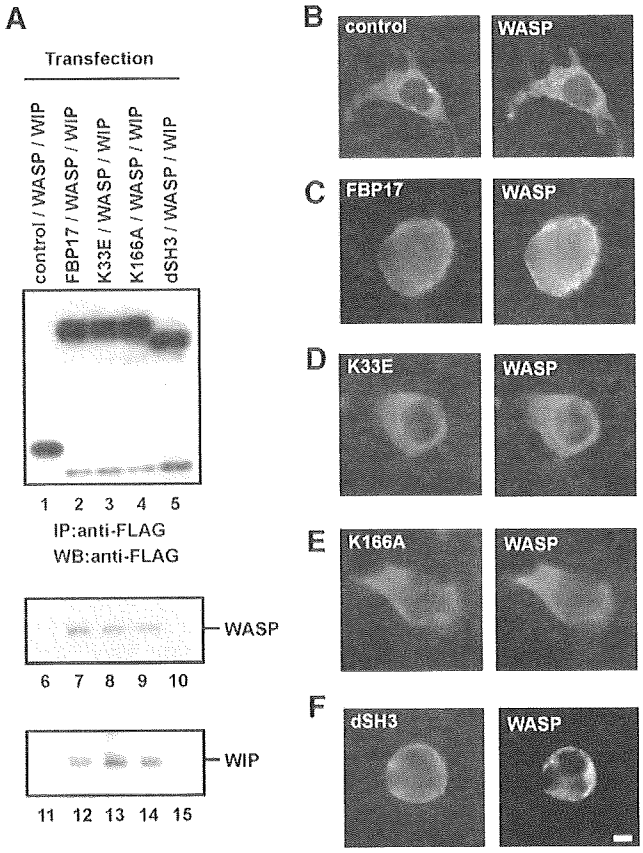

FIGURE 3. **FBP17 recruits WASP, WIP, and dynamin-2 to the plasma membrane.** *A*, HEK293 cells were co-transfected with cDNAs of the indicated FLAG-tagged proteins, Myc-tagged WASP, and HA-tagged WIP. The FLAG-tagged proteins were immunoprecipitated (*IP*) from lysates of the transfected cells with an anti-FLAG antibody followed by immunoblotting (*WB*) using antibodies to FLAG (*lanes 1–5*), WASP (*lanes 6–10*), and WIP (*lanes 11–15*). *B–F*, transfected HEK293 cells expressing FLAG-tagged proteins, Myc-WASP, and HA-WIP were double-stained with an anti-FLAG antibody and anti-WASP antibody. *B–F*, cells expressing FLAG-PDZ-GEF (*B*), FLAG-FBP17 (*C*), the FLAG-tagged FBP17 mutant with the K33E missense mutation (*D*), K166A (*E*), and the SH3-deleted FBP17 mutant dSH3 (*F*). The *bar* is 10 μm.

expressing the FLAG-tagged FBP17, K33E, and K166A constructs (Fig. 3*A*, *lanes 7–9* and *12–14*) but not the FLAG-tagged PDZ-GEF and dSH3 constructs (Fig. 3*A*, *lanes 6*, *10*, *11*, and *15*), indicating that FBP17 and its mutants K33E and K166A form a complex with WASP and WIP but that dSH3 not.

Next, cells expressing the FLAG-tagged proteins, WASP, and WIP were examined under the immunofluorescence microscope for the localization of the FLAG-tagged proteins and WASP. WASP and WIP were localized in the cytosol in cells transfected with only the WASP cDNA and only the WIP cDNA, respectively, as well as in cells expressing both WASP and WIP (supplemental Fig. 3). In cells co-expressing FLAG-PDZ-GEF (control) with WASP and WIP, both FLAG-PDZ-GEF and WASP were cytosolic (Fig. 3*B*). In cells co-expressing FLAG-FBP17 with WASP and WIP, FLAG-FBP17 localized at the plasma membrane because its EFC domain binds to the plasma membrane (Fig. 3*C*, *left panel*). In those cells, WASP also localized at the plasma membrane (Fig. 3*C*, *right panel*), indicating that FBP17 shifted the localization of WASP from the cytosol to the plasma membrane (Fig. 3, *B* and *C*). To confirm that the WASP-WIP complex was recruited to the plasma membrane, cells co-expressing FLAG-FBP17 with WASP and HA-tagged WIP were stained with an anti-FLAG monoclonal antibody and an anti-WASP polyclonal antibody or an anti-HA rat monoclonal antibody. Double staining revealed that both WASP and WIP co-localized with FLAG-FBP17 at the plasma membrane (supplemental Fig. 4, *A* and *B*). To further confirm the localization of the FBP17 mutants, cells co-expressing the FLAG-tagged FBP mutants, WASP, and WIP were stained with anti-FLAG monoclonal antibody. The K33E and K166A mutants were cytosolic and the SH3-deleted FBP17 mutant localized at the plasma membrane (supplemental Fig. 4*C*).

To determine the roles of the EFC and SH3 domains of FBP17 in this recruitment, we examined the localization of the FBP17 mutants and WASP in cells co-expressing the FBP mutants with WASP and WIP. Membrane tubulation in cells transfected with an FBP17 cDNA is an indicator of the membrane binding and deformation activities of FBP17 (18, 22). We detected *in vivo* membrane tubulation in cells expressing FBP17 and dSH3 but not in cells expressing K33E and K166A (supplemental Fig. 5). In cells co-expressing either FBP17 mutant (K33E or K166A) with WASP and WIP, both K33E and K166A were cytosolic (Fig. 3, *D* and *E*, *left panels*), and WASP was also cytosolic (Fig. 3, *D* and *E*, *right panels*). These results indicate that K33E and K166A are unable to recruit WASP to the plasma membrane, consistent with the inability of K33E and K166A to bind and deform the plasma membrane (supplemental Fig. 5).

The SH3-deleted FBP17 mutant, dSH3, localized at the plasma membrane (Fig. 3*F*, *left panel*) because its EFC domain is intact. However, WASP was cytosolic in cells co-expressing dSH3 with WASP and WIP (Fig. 3*F*, *right panel*), consistent with the inability of the dSH3 mutant to bind to WASP and WIP (Fig. 3*A*, *lanes 5*, *10*, and *15*).

To quantify the recruitment, we scored the percentage of cells in which WASP and WIP were localized at the plasma membrane. Cells expressing the FBP17 mutants (K33E, K166A, or dSH3) exhibited significantly lower plasma membrane localization of WASP and WIP than cells expressing FBP17 ($p < 0.05$; supplemental Fig. 6, *A* and *B*). FBP17 also recruited dynamin-2 to the plasma membrane, and both EFC and SH3 domains are necessary for this recruitment (supplemental Fig. 6*C*), as reported previously (18, 21). To confirm the localization of FBP17 and its mutants in cells co-expressing FBP17 with WASP, WIP, and dynamin-2, the transfected cells were stained with anti-FLAG monoclonal antibody. The wild-type FBP17 and dSH3 localized at the plasma membrane and the FLAG-PDZ-GEF (control) and the FBP mutants (K33E and K166A) were cytosolic (supplemental Fig. 6*D*).

Subcellular Localization of FBP17, WASP, WIP, and Dynamin-2 in Macrophages—To determine whether WASP, WIP, and dynamin-2 are recruited to the plasma membrane in macrophages when podosomes and phagocytic cups are formed, we examined the subcellular localization of FBP17, WASP, WIP, and dynamin-2 in macrophages forming podosomes or phagocytic cups. The cytosolic and membrane fractions were prepared from macrophages and analyzed by immunoblotting. Caspase-3 is a cytosolic marker, and sodium

potassium ATPase is a plasma membrane marker (26). FBP17 was detected in the membrane fraction from macrophages forming podosomes (Fig. 4*A*, *lane 9*). WASP, WIP, and dynamin-2 were also detected in the membrane fraction, although they are cytosolic proteins (Fig. 4*A*, *lanes 12, 15,* and *18*). FBP17 was detected in the membrane fraction from macrophages forming phagocytic cups (Fig. 4*B*, *lane 9*). WASP, WIP, and dynamin-2 were also detected in the membrane fractions from macrophages forming phagocytic cups (Fig. 4*B*, *lanes 12, 15,* and *18*). These results, taken together with Fig. 3, suggest that FBP17 recruits the WASP-WIP complex and dynamin-2 to the plasma membrane in macrophages and that both the EFC and the SH3 domains are necessary for this recruitment.

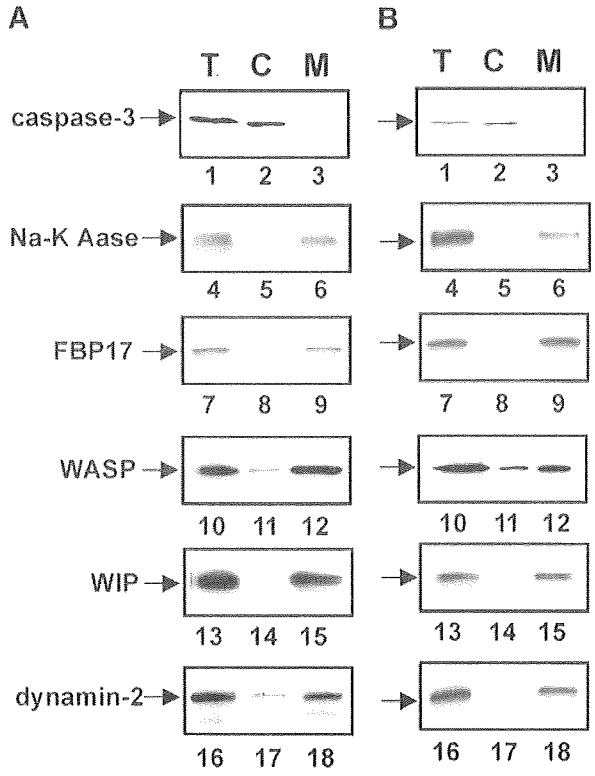

FIGURE 4. **Subcellular localization of FBP17, WASP, WIP, and dynamin-2 in macrophages.** *A*, macrophages forming podosomes. *B*, macrophages forming phagocytic cups. Total lysates (*T*), the cytosolic fraction (C), and the membrane fraction (*M*) prepared from macrophages forming podosomes (*A*) or phagocytic cups (*B*) were analyzed by immunoblotting for caspase-3 (*lanes 1–3*), sodium potassium ATPase (*Na-K Aase*; *lanes 4–6*), FBP17 (*lanes 7–9*), WASP (*lanes 10–12*), WIP (*lanes 13–15*), and dynamin-2 (*lanes 16–18*). Caspase-3 and sodium potassium ATPase (Na-K ATPase) are markers for the cytosol and plasma membrane, respectively.

The Role of Each Domain of FBP17 in the Formation of Podosomes and Phagocytic Cups—To determine the roles of the EFC and SH3 domains in the formation of podosomes and phagocytic cups, we examined whether overexpression of the FBP17 mutants affects the formation of these structures. We transfected THP-1 cells with the FBP17 constructs and confirmed the expression of FBP17 or the FBP17 mutants in transfected THP-1 cells by immunoblotting (Fig. 5*A*). When THP-1 cells were differentiated to obtain macrophage phenotypes with PMA, podosome formation was significantly reduced in cells overexpressing the K33E, K166A, and dSH3 FBP17 mutants when compared with the FBP17 wild type ($p < 0.01$; Fig. 5*B*). Phagocytic cup formation was also reduced in cells overexpressing the FBP17 mutants (Fig. 5*C*). These results indicate that the EFC domain and SH3 domain are essential for the formation of podosomes and phagocytic cups in macrophages.

Defects in Macrophages from WAS Patients—Our results suggest that the complex formation of FBP17 with WASP, WIP, and dynamin-2 at the plasma membrane is a critical step in the formation of podosomes and phagocytic cups (Figs. 1*G*, 3, and 4). In macrophages from WASP-deficient WAS patients, the complex does not form properly due to a lack of WASP expression. We examined macrophages from WASP-deficient WAS patients for the formation of podosomes and phagocytic cups. Two genetically independent WAS patients (WAS1, 211delT; and WAS2, 41–45delG) (27, 28) were assayed for the formation of those structures. Podosomes were completely absent (Fig. 6, *A–C*), and phagocytic cup formation was severely impaired (Fig. 6, *D–F*) in macrophages from both WAS patients, although FBP17, WIP, and dynamin-2 were expressed at the same level in patients as in normal individuals (Fig. 6*G*). In fact, the formation of podosomes and phagocytic cups was impaired in macrophages when the expression of WASP was reduced by siRNA transfection (4, 16). This is the first result showing that both podosome and phagocytic cup formations are defective in macrophages from WASP-deficient patients. These results are consistent with the previous observations (3, 12).

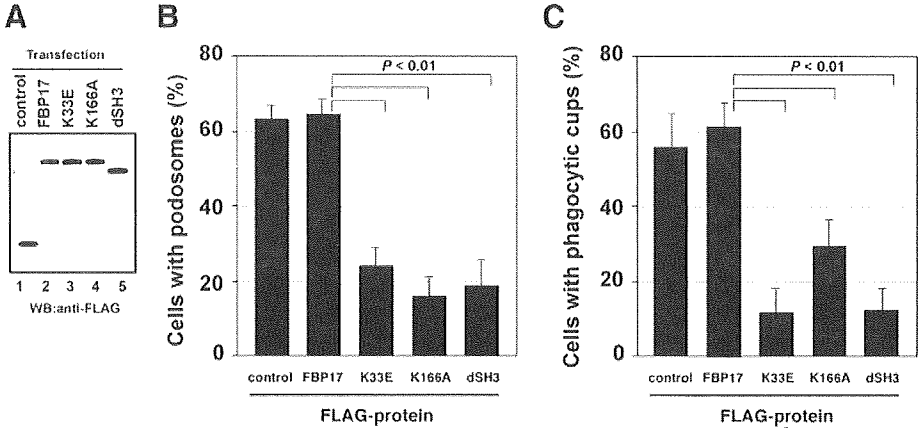

FIGURE 5. **The role of the EFC and SH3 domains of FBP17 in the formation of podosomes and phagocytic cups.** *A*, expression of FLAG-tagged proteins in transfected THP-1 cells. Total lysates prepared from transfected THP-1 cells were analyzed by immunoblotting (*WB*) using an anti-FLAG antibody. All of the FLAG-tagged proteins, FLAG-PDZ-GEF (control, *lane 1*), FLAG-FBP17 (*lane 2*), and the FBP17 mutants, K33E, K166A, and dSH3 (*lanes 3–5*) were expressed in THP-1 cells at similar levels. *B* and *C*, THP-1 cells co-transfected with cDNAs for the FLAG-tagged proteins and pmaxGFP were differentiated with PMA and then assayed for the formation of podosomes (*B*) and phagocytic cups (*C*). The percentage of cells with podosomes or phagocytic cups among all GFP-positive cells was scored. Data represent the mean ± S.D. of triplicate experiments.

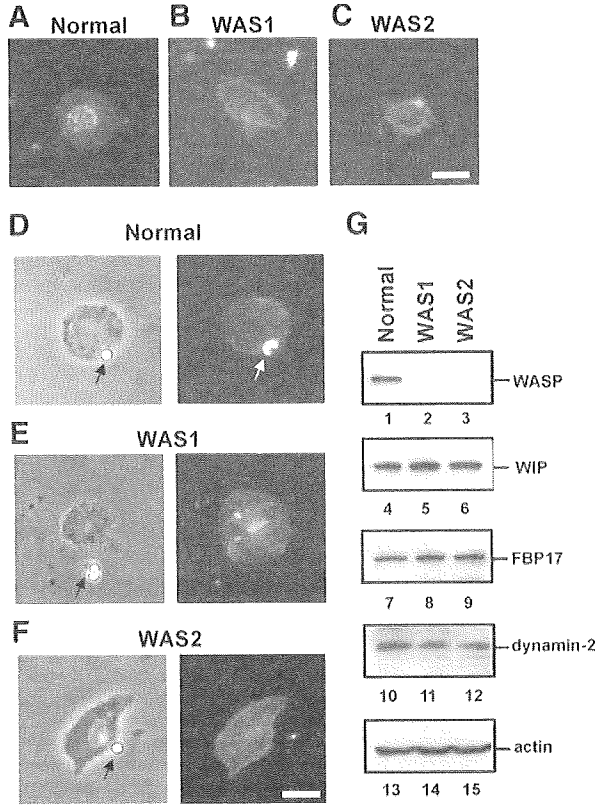

FIGURE 6. **Defective formation of podosomes and phagocytic cups in macrophages from WAS patients.** *A–F*, macrophages from a normal control and two genetically independent WAS patients (WAS1 and WAS2) were examined for the formation of podosomes (*A–C*) and phagocytic cups (*D–F*). The patients, WAS1 and WAS2, have the deletion mutations 211delT and 41–45delG, respectively, in their genomic DNAs. The *bars* are 10 μm. *G*, expression levels of WASP, WIP, FBP17, dynamin-2, and β-actin in WAS patients. Lysates prepared from macrophages from a normal control and two WAS patients (WAS1 and WAS2) were subjected to immunoblotting. WASP was not detected in the lysates from these WAS patients (*lanes 2* and *3*). Podosomes were completely absent (*A–C*) and phagocytic cup formation was severely impaired (*D–F*) in macrophages from both WAS patients, although FBP17, WIP, and dynamin-2 were expressed at the same level in patients as in normal individuals (*G*) (*lanes 4–12*).

These results give us a natural example that supports the importance of the complex formation of FBP17 with WASP, WIP, and dynamin-2 for the formation of podosomes and phagocytic cups.

DISCUSSION

Cell biological and structural analyses of the EFC domain of FBP17 have shown that the EFC domain binds to and deforms the plasma membrane (18, 22). It has previously been shown that the SH3 domain of FBP17 binds to N-WASP and dynamin in transfected cells (18, 21). However, physiologically important processes to which those activities of FBP17 contribute were unknown. Here, we have demonstrated that FBP17 recruits the WASP-WIP complex from the cytosol to the plasma membrane and that this recruitment is necessary for the formation of podosomes and phagocytic cups in macrophages. Our results suggest that FBP17 facilitates membrane deformation and actin polymerization induced by the WASP-WIP complex to occur simultaneously at the same membrane sites and that both are required for the formation of podosomes and phagocytic cups. This is supported by the observations that regulated actin polymerization is an essential process for the formation of podosomes (3) and phagocytic cups (29). Thus, FBP17 mediates a common molecular step in the formation of podosomes and phagocytic cups.

Macrophages have the ability to form both podosomes and phagocytic cups (Fig. 1, *A–D*). When macrophages having podosomes are stimulated with IgG-opsonized latex beads, the podosomes immediately disappear, and the phagocytic cups are formed at the site that the IgG beads attach. This observation indicates that the transition of the membrane structures occurs from podosomes to phagocytic cups. Macrophages migrate to sites of inflammation where they phagocytose pathogenic microbes and damaged tissue compounds and mediate local effector functions. Once macrophages encounter those materials at the site of inflammation, they stop migrating and phagocytose those materials. The transition of the macrophage functions occur from migration to phagocytosis. Podosomes and phagocytic cups are the essential membrane structures for migration and phagocytosis, respectively. Thus, the transition of the membrane structures from podosomes to phagocytic cups is essential and significant for the transition of the macrophage functions. Recently, two reports suggest that macrophage migration and phagocytosis include a common molecular mechanism to regulate actin cytoskeleton (40, 41). In this study, we identified a critical common molecular step mediated by FBP17 for the formation of podosomes and phagocytic cups, which are essential for migration and phagocytosis, respectively. In the future, elucidation of the molecular mechanisms underlying the transition would be intriguing.

It has been reported that dynamin-2 is also required for the formation of podosomes in transformed cells and osteoclasts (30–32) and phagocytic cups in a mouse macrophage cell line (33, 34) and that the FBP17-dynamin complex regulates the plasma membrane invagination (35). Our results suggest that FBP17 recruits dynamin-2 to the same site as membrane deformation and that this recruitment is also necessary for the formation of these structures (Figs. 3–5 and supplemental Fig. 6*C*). The formation of podosomes and phagocytic cups involves the process of the membrane protrusion (Fig. 1, *A–D*). The membrane protrusion requires the delivery of new membrane material (2). Our results, taken together with the above observations, suggest that dynamin-2 recruited by FBP17 to the plasma membrane probably plays an essential role in the formation of podosomes and phagocytic cups by regulating the recruitment of vesicles to the plasma membrane as new membrane material in macrophages.

Recently, the EFC domain of FBP17 was shown to bind strongly to the $PI(4,5)P_2$ (18, 22). On the other hand, it has been shown that $PI(4,5)P_2$ localizes at the podosomes in osteoclasts (36) and phagocytic cups (37, 38). These observations suggest that $PI(4,5)P_2$ is synthesized upon stimulation at the plasma membrane and plays an important role in the recruitment of FBP17 to the plasma membrane. Presumably, the $PI(4,5)P_2$ binding activity of the EFC domain is necessary for the localization of FBP17, and therefore, of the WASP-WIP complex and dynamin-2, at the sites where podosomes and phagocytic cups will form.

We suggest that the complex formation of FBP17 with WASP, WIP, and dynamin-2 at the plasma membrane is critical for the formation of podosomes and phagocytic cups (Figs. 1*G* and 3–5). In macrophages from WASP-deficient WAS patients, defects in the complex formation of FBP17 with WASP, WIP, and dynamin-2 impair the formation of podosomes and phagocytic cups (WAS1: 211delT (27); WAS2: 41–45delG(28) in Fig. 6), thereby reducing chemotaxis and phagocytosis by macrophages, which in turn would decrease the ability of host defense. The severity of WAS-associated symptoms was estimated and expressed as a score of 1–5. A score of 1 was assigned to patients with only thrombocytopenia and small platelets, and a score of 2 was assigned to patients with additional findings of mild, transient eczema or minor infections. Those with treatment-resistant eczema and recurrent infections despite optimal treatment received a score of 3 (mild WAS) or 4 (severe WAS). Regardless of the original score, if any patients then had autoimmune disease or malignancy, the score was changed to 5. The patients, WAS1 and WAS2, receive scores of 5 and 4, respectively. Both patients have the recurrent infections. We suggest that defective formation of podosomes and phagocytic cups in their macrophages (Fig. 6, *A–F*) reduces chemotaxis and phagocytosis, which are the critical processes to protect the body against infection, resulting in the recurrent infections. In addition, defective phagocytosis reduces the clearance of self-antigens such as apoptotic cells. This may cause the autoimmune diseases seen in WAS patients. In fact, Cohen *et al.* (39) recently reported that reduced clearance of apoptotic cells resulted in development of autoimmunity. Our findings therefore provide a potential mechanism for the recurrent infections and autoimmune diseases seen in WAS patients.

Acknowledgments—We thank Drs. M. Fukuda, R. C. Liddington, S. Courtneidge, A. Strongin (Burnham Institute for Medical Research), S. Grinstein (Hospital for Sich Children, Ontario, Canada), J. Condeelis (Albert Einstein Medical College), and P. De Camilli (Yale University) for critical reading of the manuscript and helpful discussion.

REFERENCES

1. Linder, S., and Aepfelbacher, M. (2003) *Trends Cell Biol.* **13,** 376–385
2. Linder, S. (2007) *Trends Cell Biol.* **17,** 107–117
3. Linder, S., Nelson, D., Weiss, M., and Aepfelbacher, M. (1999) *Proc. Natl. Acad. Sci. U. S. A.* **96,** 9648–9653
4. Tsuboi, S. (2007) *J. Immunol.* **178,** 2987–2995
5. Carman, C. V., Sage, P. T., Sciuto, T. E., Fuente, M. A. d. l., Geha, R. S., Ochs, H. D., Dvorak, H. F., Dvorak, A. M., and Springer, T. A. (2007) *Immunity* **26,** 784–797
6. Underhill, D. M., and Ozinsky, A. (2002) *Annu. Rev. Immunol.* **20,** 825–852
7. Leverrier, Y., and Ridley, A. J. (2001) *Curr. Biol.* **11,** 195–199
8. Wiskott, A. (1937) *Monatsschr. Kinderheilkd.* **68,** 212–216
9. Aldrich, R. A., Steinberg, A. G., and Campbell, D. C. (1954) *Pediatrics* **13,** 133–139
10. Notarangelo, L. D., Miao, C. H., and Ochs, H. D. (2008) *Curr. Opin. Hematol.* **15,** 30–36
11. Derry, J. M., Ochs, H. D., and Francke, U. (1994) *Cell* **78,** 635–644; Correction (1994) *Cell* **79,** 922
12. Lorenzi, R., Brickell, P. M., Katz, D. R., Kinnon, C., and Thrasher, A. J. (2000) *Blood* **95,** 2943–2946
13. Ramesh, N., Anton, I. M., Hartwig, J. H., and Geha, R. S. (1997) *Proc. Natl. Acad. Sci. U. S. A.* **94,** 14671–14676
14. Anton, I. M., de la Fuente, M. A., Sims, T. N., Freeman, S., Ramesh, N., Hartwig, J. H., Dustin, M. L., and Geha, R. S. (2002) *Immunity* **16,** 193–204
15. Chou, H. C., Anton, I. M., Holt, M. R., Curcio, C., Lanzardo, S., Worth, A., Burns, S., Thrasher, A. J., Jones, G. E., and Calle, Y. (2006) *Curr. Biol.* **16,** 2337–2344
16. Tsuboi, S., and Meerloo, J. (2007) *J. Biol. Chem.* **282,** 34194–34203
17. Tsuboi, S., Nonoyama, S., and Ochs, H. D. (2006) *EMBO Rep.* **7,** 506–511
18. Tsujita, K., Suetsugu, S., Sasaki, N., Furutani, M., Oikawa, T., and Takenawa, T. (2006) *J. Cell Biol.* **172,** 269–279
19. Chan, D. C., Bedford, M. T., and Leder, P. (1996) *EMBO J.* **15,** 1045–1054
20. Ho, H. Y., Rohatgi, R., Lebensohn, A. M., Le, M., Li, J., Gygi, S. P., and Kirschner, M. W. (2004) *Cell* **118,** 203–216
21. Kamioka, Y., Fukuhara, S., Sawa, H., Nagashima, K., Masuda, M., Matsuda, M., and Mochizuki, N. (2004) *J. Biol. Chem.* **279,** 40091–40099
22. Shimada, A., Niwa, H., Tsujita, K., Suetsugu, S., Nitta, K., Hanawa-Suetsugu, K., Akasaka, R., Nishino, Y., Toyama, M., Chen, L., Liu, Z. J., Wang, B. C., Yamamoto, M., Terada, T., Miyazawa, A., Tanaka, A., Sugano, S., Shirouzu, M., Nagayama, K., Takenawa, T., and Yokoyama, S. (2007) *Cell* **129,** 761–772
23. Auwerx, J. (1991) *Experientia (Basel)* **47,** 22–31
24. Kakimoto, T., Katoh, H., and Negishi, M. (2006) *J. Biol. Chem.* **281,** 29042–29053
25. Rebhun, J. F., Castro, A. F., and Quilliam, L. A. (2000) *J. Biol. Chem.* **275,** 34901–34908
26. Takayama, S., Krajewski, S., Krajewska, M., Kitada, S., Zapata, J. M., Kochel, K., Knee, D., Scudiero, D., Tudor, G., Miller, G. J., Miyashita, T., Yamada, M., and Reed, J. C. (1998) *Cancer Res.* **58,** 3116–3131
27. Jin, Y., Mazza, C., Christie, J. R., Giliani, S., Fiorini, M., Mella, P., Gandellini, F., Stewart, D. M., Zhu, Q., Nelson, D. L., Notarangelo, L. D., and Ochs, H. D. (2004) *Blood* **104,** 4010–4019
28. Imai, K., Morio, T., Zhu, Y., Jin, Y., Itoh, S., Kajiwara, M., Yata, J., Mizutani, S., Ochs, H. D., and Nonoyama, S. (2004) *Blood* **103,** 456–464
29. May, R. C., Caron, E., Hall, A., and Machesky, L. M. (2000) *Nat. Cell Biol.* **2,** 246–248
30. Ochoa, G. C., Slepnev, V. I., Neff, L., Ringstad, N., Takei, K., Daniell, L., Kim, W., Cao, H., McNiven, M., Baron, R., and De Camilli, P. (2000) *J. Cell Biol.* **150,** 377–389
31. McNiven, M. A., Baldassarre, M., and Buccione, R. (2004) *Front. Biosci.* **9,** 1944–1953
32. Bruzzaniti, A., Neff, L., Sanjay, A., Horne, W. C., De Camilli, P., and Baron, R. (2005) *Mol. Biol. Cell* **16,** 3301–3313
33. Gold, E. S., Underhill, D. M., Morrissette, N. S., Guo, J., McNiven, M. A., and Aderem, A. (1999) *J. Exp. Med.* **190,** 1849–1856
34. Tse, S. M., Furuya, W., Gold, E., Schreiber, A. D., Sandvig, K., Inman, R. D., and Grinstein, S. (2003) *J. Biol. Chem.* **278,** 3331–3338
35. Itoh, T., Erdmann, K. S., Roux, A., Habermann, B., Werner, H., and De Camilli, P. (2005) *Dev. Cell* **9,** 791–804
36. Chellaiah, M. A. (2005) *J. Biol. Chem.* **280,** 32930–32943
37. Botelho, R. J., Teruel, M., Dierckman, R., Anderson, R., Wells, A., York, J. D., Meyer, T., and Grinstein, S. (2000) *J. Cell Biol.* **151,** 1353–1368
38. Dewitt, S., Tian, W., and Hallett, M. B. (2006) *J. Cell Sci.* **119,** 443–451
39. Cohen, P. L., Caricchio, R., Abraham, V., Camenisch, T. D., Jennette, J. C., Roubey, R. A., Earp, H. S., Matsushima, G., and Reap, E. A. (2002) *J. Exp. Med.* **196,** 135–140
40. Brandt, D. T., Marion, S., Griffiths, G., Watanabe, T., Kaibuchi, K., and Grosse, R. (2007) *J. Cell Biol.* **178,** 193–200
41. Kato, M., Khan, S., d'Aniello, E., McDonald, K. J., and Hart, D. N. J. (2007) *J. Immunol.* **179,** 6052–6063
42. Calle, Y., Anton, I. M., Thrasher, A. J., and Jones, G. E. (2008) *J. Microsc. (Oxf.)* **231,** 494–505

Published June 1, 2009

Molecular explanation for the contradiction between systemic Th17 defect and localized bacterial infection in hyper-IgE syndrome

Yoshiyuki Minegishi,[1] Masako Saito,[1] Masayuki Nagasawa,[2] Hidetoshi Takada,[3] Toshiro Hara,[3] Shigeru Tsuchiya,[4] Kazunaga Agematsu,[5] Masafumi Yamada,[6] Nobuaki Kawamura,[6] Tadashi Ariga,[6] Ikuya Tsuge,[7] and Hajime Karasuyama[1]

[1]Department of Immune Regulation and [2]Department of Pediatrics and Developmental Biology, Graduate School, Tokyo Medical and Dental University, Tokyo 113-8519, Japan
[3]Department of Pediatrics, Graduate School of Medical Sciences, Kyushu University, Fukuoka 812-0054, Japan
[4]Department of Pediatrics, Tohoku University, Sendai 980-0872, Japan
[5]Department of Pediatrics, Shinshu University, Matsumoto 390-8621, Japan
[6]Department of Pediatrics, Hokkaido University Graduate School of Medicine, Sapporo 060-8638, Japan
[7]Department of Pediatrics, Fujita Health University, Nagoya 470-1192, Japan

Hyper-IgE syndrome (HIES) is a primary immunodeficiency characterized by atopic manifestations and susceptibility to infections with extracellular pathogens, typically *Staphylococcus aureus*, which preferentially affect the skin and lung. Previous studies reported the defective differentiation of T helper 17 (Th17) cells in HIES patients caused by hypomorphic *STAT3* mutations. However, the apparent contradiction between the systemic Th17 deficiency and the skin/lung-restricted susceptibility to staphylococcal infections remains puzzling. We present a possible molecular explanation for this enigmatic contradiction. HIES T cells showed impaired production of Th17 cytokines but normal production of classical proinflammatory cytokines including interleukin 1β. Normal human keratinocytes and bronchial epithelial cells were deeply dependent on the synergistic action of Th17 cytokines and classical proinflammatory cytokines for their production of antistaphylococcal factors, including neutrophil-recruiting chemokines and antimicrobial peptides. In contrast, other cell types were efficiently stimulated with the classical proinflammatory cytokines alone to produce such factors. Accordingly, keratinocytes and bronchial epithelial cells, unlike other cell types, failed to produce antistaphylococcal factors in response to HIES T cell–derived cytokines. These results appear to explain, at least in part, why HIES patients suffer from recurrent staphylococcal infections confined to the skin and lung in contrast to more systemic infections in neutrophil-deficient patients.

CORRESPONDENCE
Yoshiyuki Minegishi:
yminegishi.mbch@tmd.ac.jp

Abbreviations used: BD, β-defensin; CAA, *Candida albicans* antigen; CGD, chronic granulomatous disease; HIES, hyper-IgE syndrome; HMVEC-L, human lung microvascular endothelial cell; HUVEC, human umbilical vein endothelial cell; SEB, staphylococcal enterotoxin B; TLR, Toll-like receptor.

The identification of Th17 cells as a third subset of helper T cells has illuminated the fact that distinct subsets of helper T cells have been evolved to protect our body from infections by various types of microorganisms and are involved differently in the induction and exacerbation of various immunological disorders. Th17 cells are characterized and distinguished from IFN-γ–producing Th1 cells and IL-4–producing Th2 cells by their production of so-called Th17 cytokines including IL-17 (IL-17A), IL-17F, and IL-22 (1–4). For their differentiation from naive CD4 T cells, Th17 cells require different cytokines and transcription factors than do Th1, Th2, or regulatory T cells. The roles of Th17 cells in immune responses are also different from those of other helper T cells. In particular, their pathological roles in autoimmune and inflammatory diseases, including multiple sclerosis, rheumatoid arthritis, psoriasis, and inflammatory bowel diseases, have been studied extensively (5–10).

Although the functions of Th17 cells under physiological conditions have not been completely elucidated, accumulating data suggest that Th17 cells play crucial roles in the host defense against extracellular pathogens that are

The Rockefeller University Press $30.00
J. Exp. Med. Vol. 206 No. 6 1291-1301
www.jem.org/cgi/doi/10.1084/jem.20082767

Supplemental Material can be found at:
http://jem.rupress.org/cgi/content/full/jem.20082767/DC1

Published June 1, 2009

not efficiently cleared by Th1- and Th2-type immune responses. Th17-type cytokines IL-17A and IL-17F are important for the recruitment of neutrophils (11), whereas IL-22 induces the production of antimicrobial peptides β-defensin (BD) 2 and BD3 by keratinocytes, through the activation of STAT3 (12–14). Mice with a homozygous deletion of the gene encoding the IL-17RA (IL-17 receptor A) and mice that do not produce IL-22 are susceptible to lung infection by the Gram-negative bacteria *Klebsiella pneumoniae* and *Mycoplasm pulmonis* (15–17). Mice that produce neither IL-17A nor IL-17F are susceptible to skin infection by the Gram-positive bacteria *Staphylococcus aureus* (18). Administration of anti–IL-17A neutralizing antibodies impairs both the intra-abdominal abscess formation in response to *Bacteroides fragilis* and *Escherichia coli* (19–21) and the host defense against systemic infection by the fungus *Candida albicans* (22). These data indicate that Th17 cells play a key role in immune responses to extracellular bacteria and fungi in mice. In contrast, the anti-pathogenic roles of Th17 cells in humans are relatively uncertain.

Recent studies demonstrated that the differentiation of human Th17 cells was defective in patients with hyper-IgE syndrome (HIES) (23–26). HIES is a primary immunodeficiency disease caused by dominant-negative mutations in the DNA-binding domain, SH2 domain, or transactivating domain of STAT3 (26–28). As expected from the important roles of STAT3 in transducing signals for a variety of cytokines, growth factors, and hormones, patients with HIES display complex clinical manifestations in multiple organs, including atopic dermatitis with high serum IgE levels and abnormalities of the bones and teeth (29–32). Most patients suffer from recurrent infections by fungi and bacteria, predominantly the Gram-positive bacteria *S. aureus*. The presence of these infections suggests that Th17 cells play a crucial role in protection from extracellular pathogens, not only in mice but also in humans. However, curiously, the staphylococcal infections in HIES patients are often confined to the skin and lung and manifest clinically as skin abscesses and cyst-forming pneumonia. These skin- and lung-restricted infections are in sharp contrast to the pattern of infection observed in patients with a neutrophil deficiency. For example, in patients with chronic granulomatous disease (CGD), staphylococcal infections occur in a wide variety of organs including the lung, lymph nodes, skin, liver, bone, gastrointestinal tract, kidney, and brain (33). Thus, it remains elusive why HIES patients suffer from skin- and lung-restricted staphylococcal infections in spite of their systemic Th17 deficiency.

In the present study, we explored possible molecular mechanisms underlying the recurrent staphylococcal infections confined to the skin and lung in HIES patients. We found that primary human keratinocytes and bronchial epithelial cells displayed a much stronger dependence than other cell types on Th17 cytokines in their production of antistaphylococcal factors including the neutrophil-recruiting chemokines and antibacterial peptides. T cells from HIES patients, in spite of their defect in production of Th17 cytokines, showed normal production of other proinflammatory cytokines, including IL-1β, which was insufficient for triggering keratinocytes and bronchial epithelial cells but sufficient for other cell types to produce antistaphylococcal factors. Th17 cytokines and classical proinflammatory cytokines synergistically stimulated keratinocytes and bronchial epithelial cells, but the synergy was not seen in other types of cells. These findings provide a possible molecular explanation for the apparent contradiction between the systemic Th17 deficiency and the skin and lung-restricted staphylococcal infections in HIES patients.

RESULTS

HIES T cells produce little or no Th17 cytokines and fail to stimulate keratinocytes to secrete neutrophil-recruiting chemokines and BDs

We first examined the profile of cytokines produced by T cells from our cohort of HIES patients whose *STAT3* genes carried mutations. The amounts of IL-17A and IL-22 secreted from the patients' T cells upon stimulation with anti-CD3 and anti-CD28 mAbs were invariably only ~5–10% of those from healthy control subjects, which is in accordance with previous results (23–26), whereas the production levels of IFN-γ, IL-1β, and TNF-α were comparable in the two groups (Fig. 1). Real-time quantitative RT-PCR demonstrated that the up-regulation of *IL-17F* expression by the patients' T cells was also impaired (unpublished data). Thus, the patients' T cells showed a selective defect in the production of Th17 cytokines.

We next investigated the functional consequences of the Th17 deficiency in the context of staphylococcal infections of the skin. Normal human primary epidermal keratinocytes were cultured in vitro with culture supernatants from HIES patients' or control subjects' T cells that had been unstimulated or stimulated with anti-CD3 plus anti-CD28. The expression and production of two chemokines, CXCL8 (IL-8) and CCL2, was up-regulated in the keratinocytes cultured with the conditioned medium from activated control T cells (Fig. 2 A and Fig. S1). In contrast, although CCL2 was also up-regulated by the conditioned medium from activated HIES T cells, CXCL8 was not (Fig. 2 A and Fig. S1). Among the three antimicrobial peptides (BDs) examined, at the mRNA and protein level the expression of BD1 but not BD2 or BD3 was up-regulated in keratinocytes when they were stimulated with conditioned medium from the T cells of HIES patients, but all three were up-regulated by the conditioned medium from the control subjects' T cells (Fig. 2 A and Fig. S1). Thus, the HIES patients' T cells could not stimulate keratinocytes to produce a significant amount of the neutrophil-recruiting chemokine CXCL8 or the antimicrobial peptides BD2 and BD3, but they could stimulate the up-regulation of CCL2 and BD1.

T cell–derived Th17 cytokines are responsible for the production of CXCL8 and BDs from keratinocytes

When the supernatants from activated control T cells were treated with the combination of anti–IL-17A and anti–IL-22 blocking mAbs before incubation with keratinocytes, their capability of stimulating keratinocytes to up-regulate CXCL8, BD2, and BD3 was diminished to the level displayed by the

Published June 1, 2009

HIES patients' T cells (Fig. 2 A and Fig. S1). Either anti–IL-17A or anti–IL-22 alone was less effective than their combination (Fig. S2). Thus, the defective production of chemokines and BDs by keratinocytes in response to the conditioned medium from the patients' T cells was attributable to the T cells' defective production of Th17 cytokines.

We next examined the direct effect of the keratinocyte-derived factors on the growth of *Staphylococcus aureus* using a colony-forming assay (Fig. 2, B and C). When bacteria were cultured with the culture supernatant from keratinocytes stimulated by control T cells, the number of bacterial colonies was reduced to 60% as compared with that when cultured with control medium. However, this was not the case when HIES T cells were used to stimulate keratinocytes. The antibacterial activity was completely abrogated when the culture supernatant from the control T cells was pretreated with the blocking mAbs for IL-17A and IL-22 before it was added to the keratinocytes (Fig. 2 B), and it was attenuated when the keratinocyte supernatants were pretreated with an anti-BD3 mAb before their application to the bacterial culture (Fig. 2 C). These results indicated that control but not HIES T cells produced Th17 cytokines that, in turn, acted on keratinocytes to elicit their secretion of antimicrobial factors including BD3.

Keratinocytes and bronchial epithelial cells display a greater dependence on Th17 cytokines for their production of chemokines and BDs than other cell types

To learn why the staphylococcal infections are confined to the skin and lung in HIES patients, we analyzed different lineages of human primary cells for their ability to secrete chemokines and BDs in response to T cell–derived factors including Th17 cytokines. We first compared their responsiveness to culture supernatants from either control or patient T cells that were activated with anti-CD3 and anti-CD28 mAbs. Primary bronchial epithelial cells responded to the T cell conditioned medium just as the primary keratinocytes did. That is, both cell types up-regulated the expression and production of chemokines (CXCL8 and CXCL1) and BDs (BD2 and BD3) when incubated with the supernatants from control T cells but not from HIES T cells (Fig. 3 A and Fig. S3). Interestingly, primary dermal fibroblasts, human umbilical vein endothelial cells (HUVEC), and human lung microvascular endothelial cells (HMVEC-L) responded equally well, in terms of their secretion of the chemokines and BDs, to the supernatants from control or patient T cells (Fig. 3 A and Fig. S3). This was also true for the expression and production of CXCL8 and CXCL1 by human macrophages (Fig. 3 A and Fig. S3). Human macrophages did not produce detectable amounts of BDs. Thus, keratinocytes and bronchial epithelial cells responded differently to T cell–derived factors than the other cell types tested and appeared to be much more dependent on Th17 cytokines for their induction to secrete chemokines and BDs.

These findings prompted us to examine the responses of different cell types to individual cytokines and their combinations, including the Th17 cytokines (IL-17A, IL-17F, and IL-22), classical proinflammatory cytokines (IL-1β, TNF-α, and IFN-γ), or both. Keratinocytes secreted CXCL8 in response to IL-17A, IL-22, IL-1β, or TNF-α in a dose-dependent

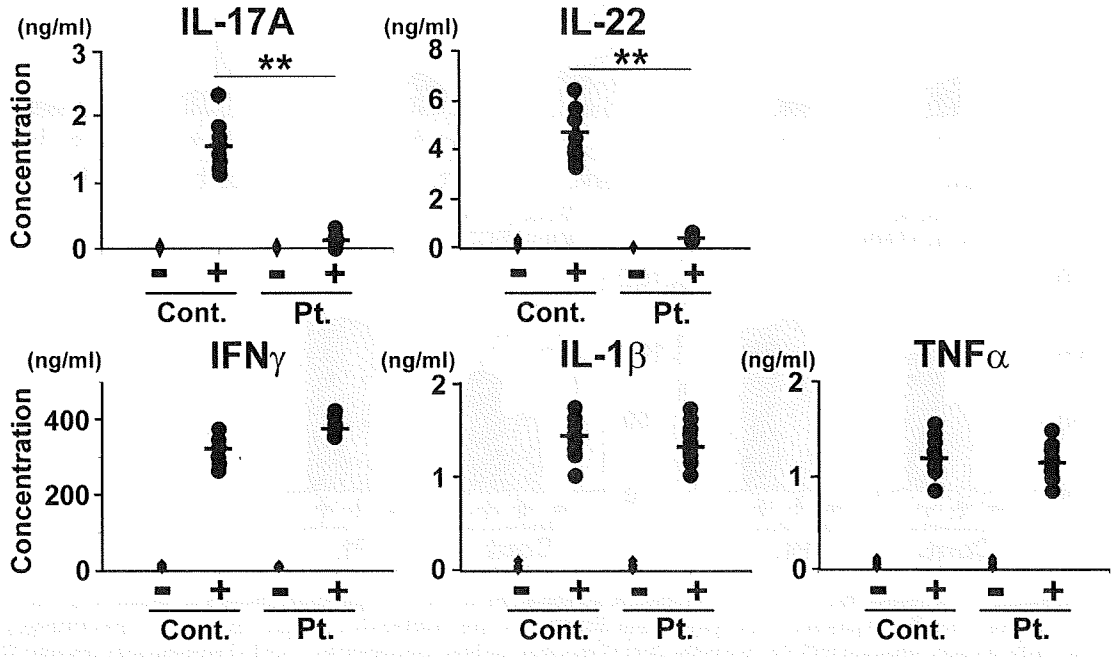

Figure 1. HIES T cells produce greatly reduced amounts of Th17 cytokines and normal amounts of classical proinflammatory cytokines upon activation. PBMCs from HIES patients (Pt.) and control subjects (Cont.; $n = 8$ each, indicated by dots) were stimulated (+) or not (−) with anti-CD3 and anti-CD28 for 72 h, and the concentration of the indicated cytokines in their culture supernatants was determined by ELISA. The results shown are representative of three independent experiments. **, $P < 0.01$.

Published June 1, 2009
JEM

manner, but they responded poorly to IL-17F and IFN-γ (Fig. S4 A). Using the Th17 cytokine cocktail or the classical proinflammatory cytokine cocktail resulted in some additive effect on the keratinocytes' secretion of CXCL8 (Fig. S4, B and C). In contrast, the combination of both types of cytokines dramatically enhanced the CXCL8 production by the keratinocytes (Fig. 3 B and Fig. S5). This was also the case for bronchial epithelial cells (Fig. 3 B). In contrast, fibroblasts, HUVEC, and HMVEC-L secreted a large quantity of CXCL8 in response to the classical proinflammatory cytokine cocktail, but the further addition of Th17 cytokine cocktail caused no significant enhancement of CXCL8 production (Fig. 3 B). Furthermore, the Th17 cytokine cocktail was much less effective in stimulating fibroblasts, HUVEC, and HMVEC-L than the classical cytokine cocktail, and the amount of CXCL8 produced by the Th17 cytokine cocktail-treated fibroblasts, HUVEC, and HMVEC-L was ~10–30% of that produced by stimulation with the classical proinflammatory cocktail. Macrophages responded to the cytokines in a pattern similar to fibroblasts, HUVEC, and HMVEC-L, although the macrophages produced 10× less CXCL8 than the others.

In keratinocytes and bronchial epithelial cells, the marked synergy caused by combining the Th17 and classical proinflammatory cytokines affected not only the expression of CXCL8 but also that of other chemokines (CXCL1 and CXCL2) and BDs (BD2 and BD3; Fig. S6 A). In accordance with this finding, the supernatants of keratinocytes stimulated with the Th17–classical cytokine combination caused robust neutrophil chemotaxis compared with the supernatants from keratinocytes stimulated with only one of the cocktails (Fig. S6 B).

Previous studies demonstrated that the stimulation of keratinocytes with toll-like receptor (TLR) 2 ligands induces the production of the chemokines and antimicrobial peptides (34, 35). In agreement with this, the keratinocytes showed up-regulated CXCL8 secretion and BD expression in response to lipoteichoic acid, peptidoglycan, or fixed *S. aureus*, but the extent of up-regulation was <10% of that observed after stimulation with the combination of Th17 and proinflammatory cytokines (Fig. S6 C).

Molecular mechanisms underlying the unique responsiveness of keratinocytes and bronchial epithelial cells to Th17 cytokines in synergy with other proinflammatory cytokines

To explore the possible molecular basis of the poorer response of keratinocytes and bronchial epithelial cells to the

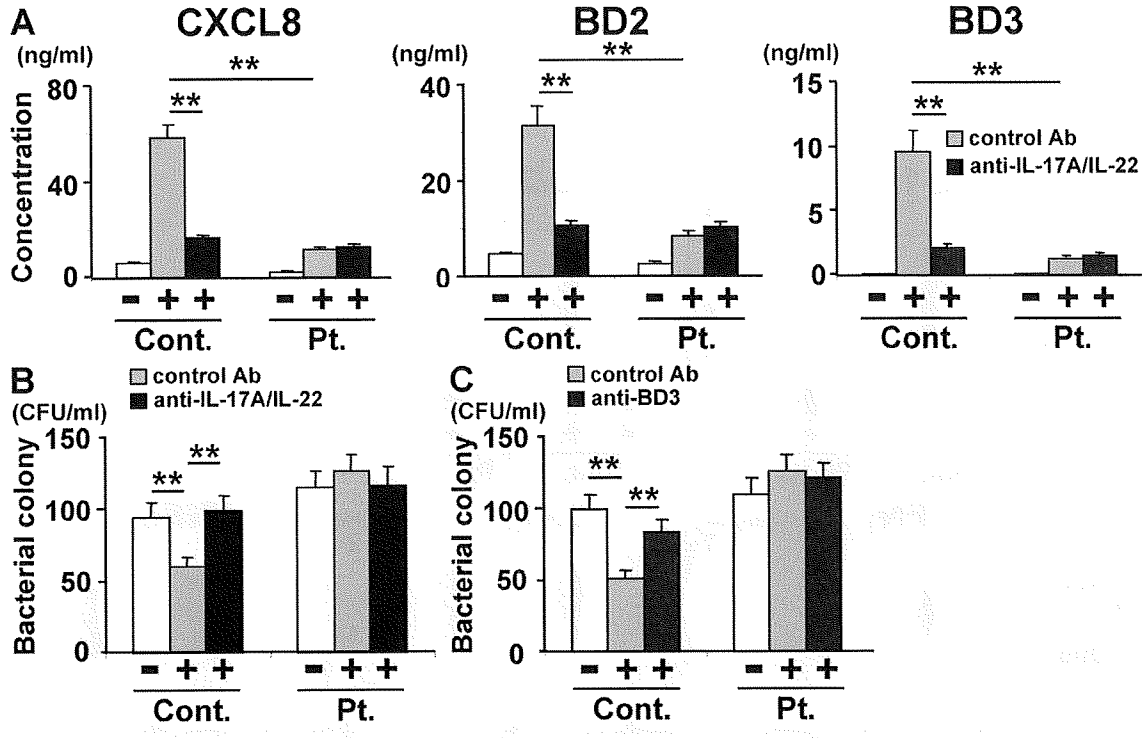

Figure 2. Supernatants of activated HIES T cells fail to stimulate keratinocytes to secrete significant amounts of antibacterial factors. In the presence or absence of anti-IL-17A plus anti-IL-22 (A and B), anti-BD3 (C), or isotype-matched control antibodies, primary human keratinocytes were incubated for 48 h with the supernatants of HIES (Pt.) or control (Cont.) T cells that had been stimulated (+) or not (−) with anti-CD3 and anti-CD28 for 72 h as in Fig. 1. (A) The concentration of CXCL8, BD2, and BD3 in keratinocytes supernatants was determined by ELISA. Representative data from one patient and one control are shown (mean ± SD; $n = 3$), and similar results were obtained from the other patients and controls. (B and C) The culture supernatants of keratinocytes were analyzed for their antistaphylococcal activity by the colony assay (mean ± SD; $n = 3$). The results shown in are representative of at least three independent experiments. **, $P < 0.01$.

Published June 1, 2009

classical proinflammatory cytokines, as compared with the other types of cells, we analyzed the expression of the classical cytokine IL-1R1 (IL-1 receptor) and its antagonists IL-1R2 and IL-1Ra (Fig. 4, A and B). Compared with fibroblasts, keratinocytes expressed 1/600th of IL-1R1 transcripts, 170-fold more IL-1Ra transcripts, and 260-fold more IL-1R2 (Fig. 4 A). The great difference in their expression between keratinocytes and fibroblasts was also confirmed at the protein level (Fig. 4 B). Bronchial epithelial cells showed the keratinocyte-type expression, whereas HUVEC and HMVEC-L displayed the fibroblast-type expression (Fig. 4 A and not depicted). Consistent with this result, keratinocytes showed a much poorer up-regulation of c-Fos and IL-6 than fibroblasts in response to IL-1β (Fig. 4 C). This appeared to partly explain why keratinocytes and bronchial epithelial cells were less sensitive to the classical proinflammatory cytokines than fibroblasts but did not account for the strong synergy between the Th17 and the classical proinflammatory cytokines in the keratinocytes. Therefore, we next examined the possible cross-talk between the two types of cytokines in terms of the regulation of cytokine receptor expression.

We found that the expression of the Th17 cytokine receptors IL-17RA, IL-17RC, and IL-22R was up-regulate, in keratinocytes incubated with the classical proinflammatory

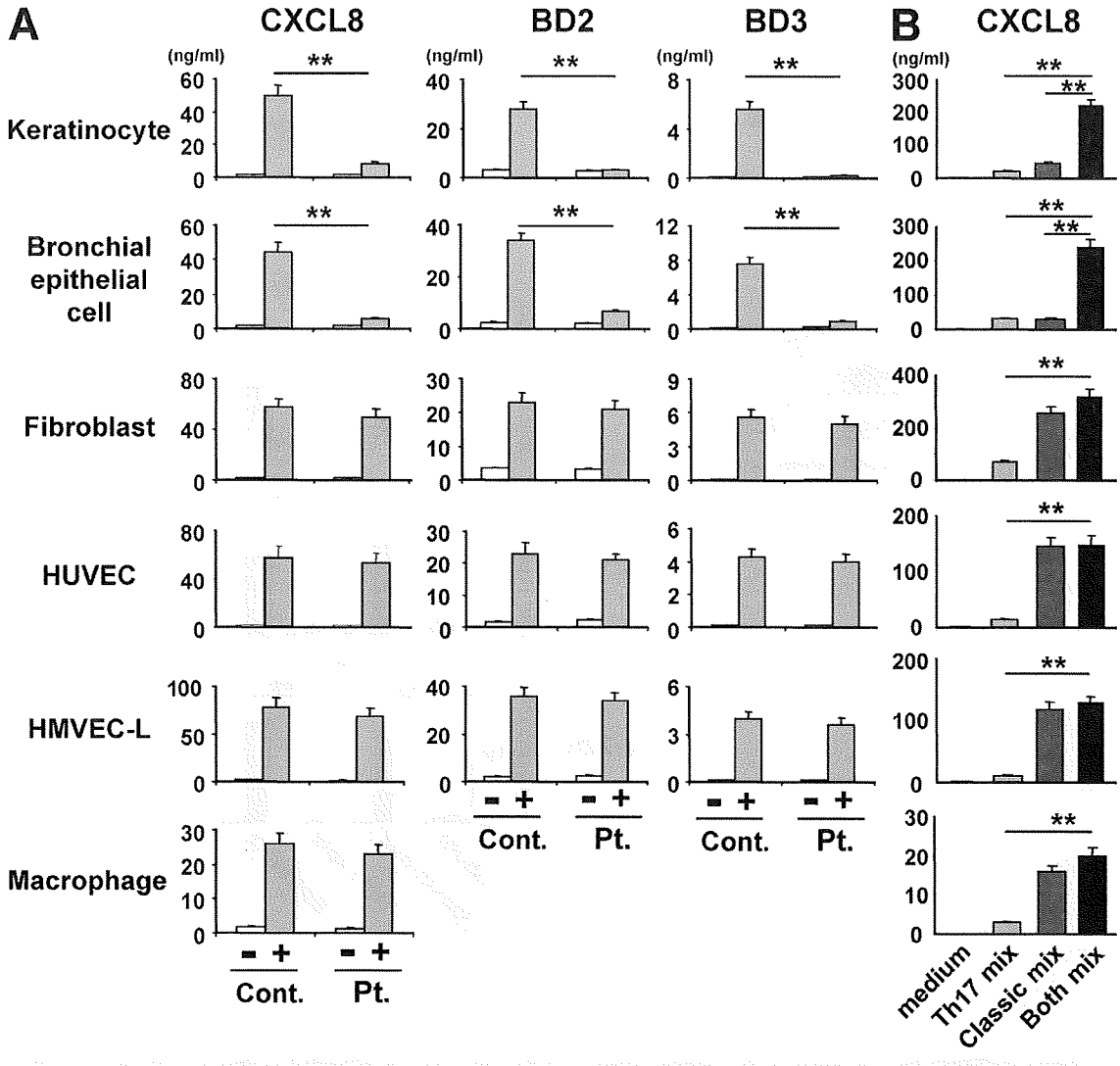

Figure 3. Keratinocytes and bronchial epithelial cells show greater dependence on Th17 cytokines for the production of chemokines and BDs than other cell types. Primary human keratinocytes, bronchial epithelial cells, dermal fibroblasts, endothelial cells (HUVEC and HMVEC-L), and macrophages were incubated for 48 h with T cell supernatants that were prepared as described in Fig. 1 A or with the Th17 cytokine cocktail (Th17 mix: IL-17A + IL-17F + IL-22), the classical proinflammatory cytokine cocktail (classical mix: TNF-α + IL-1β + IFN-γ), or the combination of both (both mix; B). The concentration of CXCL8, BD2, and BD3 in their culture supernatants was determined by ELISA. Representative data from one patient and one control are shown in A (mean ± SD; $n = 3$), and similar results were obtained from the other patients and controls. The results shown are representative of at least three independent experiments. **, $P < 0.01$.

Published June 1, 2009

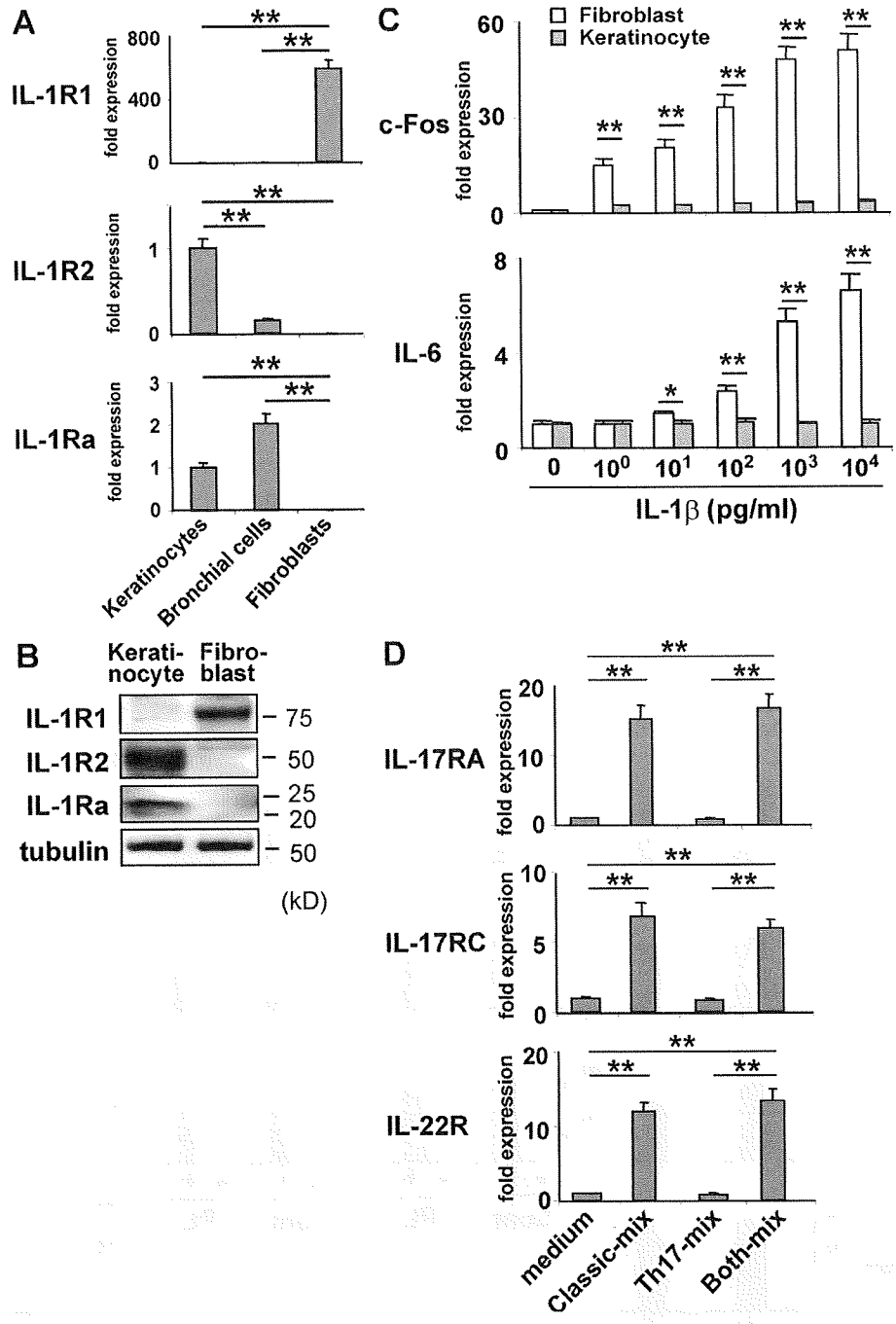

Figure 4. Distinct expression and regulation of the cytokine receptors in keratinocytes and fibroblasts compared with those in other cell types. (A) The expression of *IL-1R1*, *IL-1Ra*, and *IL-1R2* in the indicated cells was determined by quantitative RT-PCR. Data shown were normalized to *HPRT* levels, and the level of expression in keratinocytes was defined as 1.0. (B) IL-1R1, IL-1R2, and IL-1Ra proteins in keratinocytes and fibroblasts were detected by immunoblotting. (C) Keratinocytes and fibroblasts were cultured for 15 min with the indicated concentration of IL-1β and analyzed by quantitative RT-PCR for the expression of *c-Fos* and *IL-6*. Data shown were normalized to HPRT levels, and the level of expression in cells cultured without IL-1β was defined as 1.0 for each cell type. (D) Keratinocytes cultured as in Fig. 3 B were analyzed by quantitative RT-PCR for the expression of *IL-17RA*, *IL-17RC*, and *IL-22R*. The data shown were normalized to the *HPRT* levels, and the level of expression in cells cultured without any added cytokine was defined as 1.0. The results shown are representative of three independent experiments. Error bars show mean ± SD ($n = 3$). *, $P < 0.05$; **, $P < 0.01$.

Published June 1, 2009

cytokines but not the Th17 cytokines (Fig. 4 D and Fig. S7). Conversely, in keratinocytes incubated with the Th17 cytokines, the expression of the receptors for the classical proinflammatory cytokines was up-regulated, albeit less markedly (unpublished data). This reciprocal up-regulation of cytokine receptor expression was also observed in bronchial epithelial cells (unpublished data). These findings could account, at least in part, for the synergistic effect of the Th17 and the classical proinflammatory cytokines on the production of antibacterial factors by keratinocytes and bronchial epithelial cells.

HIES T cells show poor ability of stimulating keratinocytes in response to staphylococcal superantigens and candida antigens

We next investigated the responses of HIES T cells under more clinically relevant conditions to obtain a better insight into the susceptibility to staphylococcal infections observed in HIES patients. When stimulated with the *S. aureus*–derived superantigens for T cells, staphylococcal enterotoxin B (SEB), HIES patients' T cells produced drastically reduced amounts of IL-17A and IL-22, <10% of those produced by control T cells (Fig. 5 A). In contrast, the IL-1β production was normal, and the IFN-γ and TNF-α production was even enhanced in SEB-stimulated HIES T cells (Fig. 5 A). It is of note that the supernatants of SEB-stimulated HIES T cells showed much poorer ability to induce the production of CXCL8 and BD2 in keratinocytes compared with those from control T cells (Fig. 5 B). In contrast, both supernatants from HIES and control T cells almost equally well stimulated fibroblasts to produce CXCL8 and BD2. The combination of anti–IL-17A and –IL-22 efficiently inhibited the CXCL8/BD2-inducing activity of control T cells' supernatants in keratinocytes but showed no significant inhibition in the CXCL8/BD2 production from fibroblasts that were stimulated with the supernatants from either control or HIES T cells (Fig. 5 B). These results strongly suggested that Th17

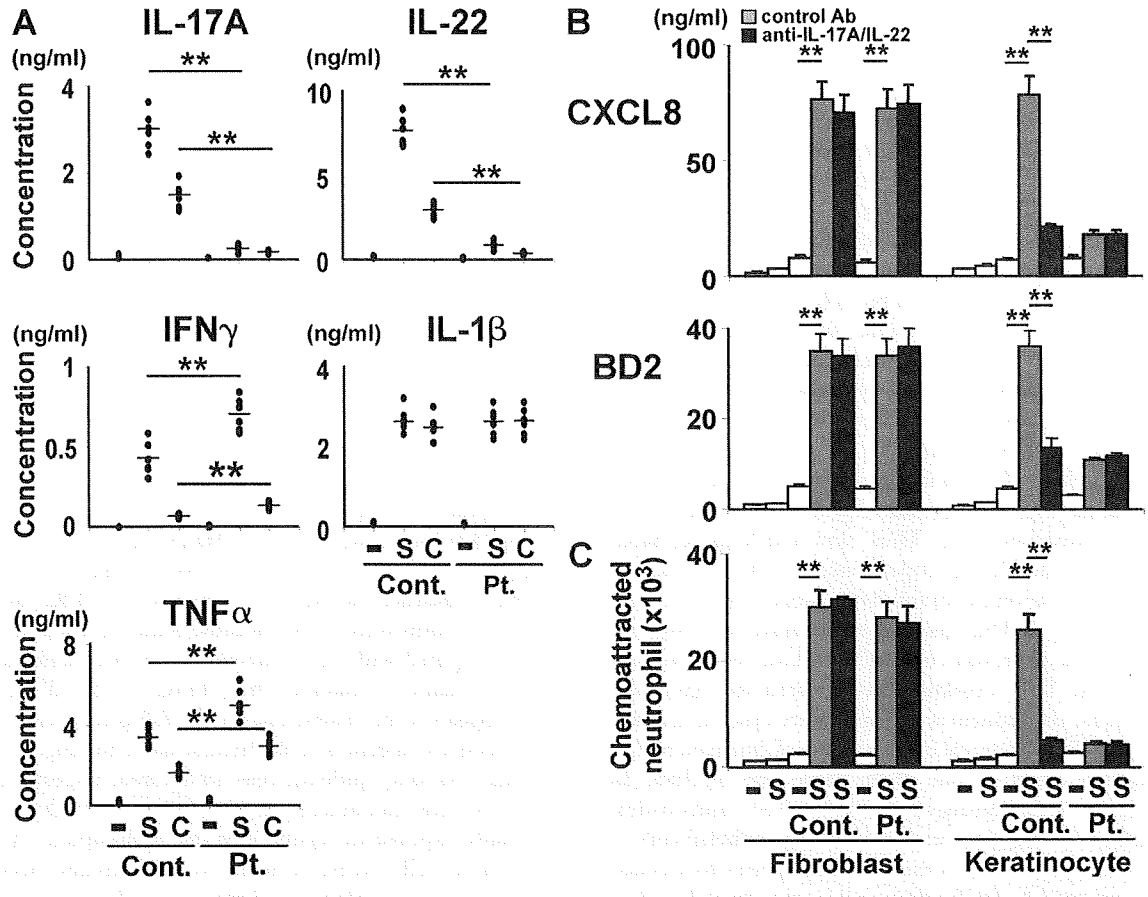

Figure 5. HIES T cells show poor ability of stimulating keratinocytes in response to staphylococcal superantigens and candida antigens. (A) PBMCs from HIES patients (Pt.) and control subjects (Cont.; $n = 6$ each, indicated by dots) were stimulated or not (−) with SEB (S, 100 ng/ml) or CAA (C, 1/20,000 vol/vol) for 5 d, and the concentration of the indicated cytokines in their culture supernatant was determined by ELISA. (B and C) Fibroblasts and keratinocytes were cultured for 48 h in the absence (−) or presence (S) of SEB or with the supernatants of patients (Pt.) or control (Cont.) PBMCs that had been unstimulated (−) or stimulated with SEB (S) as in A, in the presence or absence of anti–IL-17A + anti–IL-22 or isotype-matched control antibodies. Their culture supernatants were analyzed by ELISA for the secretion of CXCL8 and BD2 (B) and evaluated for their neutrophil chemotactic activity (C). The results shown are representative of two independent experiments. Error bars show mean ± SD ($n = 3$). **, $P < 0.01$.

Published June 1, 2009

cytokines secreted by SEB-stimulated T cells played a critical role in the induction of CXCL8 and BD2 production in keratinocytes but not in fibroblasts. In accord with these results, supernatants of keratinocytes stimulated with HIES T cells showed little or no ability of neutrophil chemoattraction, whereas those of keratinocytes stimulated with control T cells and those of fibroblasts stimulated with either control or HIES T cells induced robust neutrophil chemotaxis (Fig. 5 C). These in vitro findings may account in part, if not entirely, for the skin/lung-confined susceptibility to staphylococcal infections observed in HIES patients.

We further examined the responsiveness of HIES T cells to *Candida albicans* antigen (CAA). HIES T cells showed impaired cytokine production in response to CAA in the essentially same pattern as observed in response to SEB (Fig. 5 A). This may also explain in part the incidence of mucocutaneous infections with *C. albicans* that is often observed in HIES patients.

DISCUSSION

In the present study, we demonstrated that skin and lung epithelial cells displayed an unusual pattern of responsiveness to Th17 and other proinflammatory cytokines that was distinct from that of the other cell types tested. This previously unrecognized modes of cytokine responses could fill in the apparent gap between the systemic Th17 deficiency and the tissue-dependent susceptibility to staphylococcal infections in the HIES patients. Both Th17 cytokines and other classical proinflammatory cytokines stimulate a variety of cells to produce neutrophil-recruiting chemokines and antimicrobial peptides, which are important for providing protection against bacterial infections (7). We found that skin and lung epithelial cells efficiently secreted antibacterial factors only when stimulated with a combination of Th17 cytokines and classical proinflammatory cytokines. These observations were made using primary cells that were grown on plastic. In contrast, fibroblasts, endothelial cells, and macrophages efficiently secreted antibacterial factors when stimulated with the classical proinflammatory cytokines alone. Thus, skin and lung epithelial cells showed a much higher dependence on Th17 cytokines, in synergy with the classical proinflammatory cytokines, than the other cell types. The classical proinflammatory cytokines up-regulated the expression of Th17 cytokine receptors and, conversely, the Th17 cytokines up-regulated the expression of receptors for the classical proinflammatory cytokines, albeit less strongly. This reciprocal up-regulation of cytokine receptor expression could be one of the molecular mechanisms underlying the strong synergy between the Th17 and classical proinflammatory cytokines in skin and lung epithelial cells.

This synergistic action of the cytokines appears to account in part, if not entirely, for the skin- and lung-restricted staphylococcal infections of HIES patients. *S. aureus* produces enterotoxins, including SEB, that function as superantigens to stimulate the bulk of T cells. The HIES patients' T cells showed impaired production of Th17 cytokines in response to SEB but normal production of the classical proinflammatory cytokines. Therefore, the skin and lung epithelial cells of HIES patients, unlike other cell types, probably do not secrete sufficient amounts of neutrophil-recruiting chemokines and the antimicrobial peptide BDs to fend off staphylococcal infection. With regard to the sites of bacterial infections, it is important to consider the pathogen's characteristics. The tendency of *S. aureus* to colonize the skin and upper respiratory tract may explain the skin/lung-restricted staphylococcal infections observed in HIES patients. It is of note, however, that CGD patients suffer from staphylococcal infections that occur in a wide variety of organs, including the lung, lymph nodes, skin, liver, bone, gastrointestinal tract, kidney, and brain (33). The difference in the spectrum of affected tissues between HIES and CGD patients strongly suggests that the host factors, in addition to the pathogen's intrinsic factors, would determine the preferential sites of infections. In HIES patients, unlike in CGD patients, the neutrophils themselves are normal in their number and function; however, they probably cannot be recruited to the skin and lung because HIES T cells cannot induce the skin and lung epithelial cells to produce neutrophil-recruiting chemokines like CXCL8, even though we cannot formally exclude the possibility that the STAT3 mutation in the epithelial cells of HIES patients also contributes to impaired production of antistaphylococcal factors including CXCL8. Mice deficient for IL-17RA or IL-22 and mice treated with an anti–IL-17A blocking antibody are susceptible to infections with Gram-negative bacteria, such as *K. pneumoniae*, *M. pulmonis*, *B. fragilis*, *E. coli*, and *Citrobacter rodentium*, which are rarely observed in HIES patients (16, 17, 20, 21, 36, 37). The reason for this difference between human and mouse in bacterial susceptibility remains to be determined.

TLR-mediated signals are known to be important for immune protection from staphylococcal infections. The outer cell wall of *Staphylococcus aureus* is composed of exposed peptidoglycan and lipoteichoic acid, which are recognized by TLR2 (38–40). Mice deficient in TLR2 and patients deficient in IRAK4, a transducer of TLR signaling, show increased susceptibility to staphylococcal infections (41–43). Importantly, TLR2 signaling is intact in HIES patients (44, 45). We demonstrated in the present study that keratinocytes indeed produced antibacterial factors in response to TLR2 ligands, but the amounts were <10% of those induced when the cells were stimulated with the combination of Th17 and classical proinflammatory cytokines. Thus, TLR2-mediated signaling alone appears to be insufficient for the full protection against staphylococcal infection of the human skin and lung.

Skin and lung epithelial cells are located, respectively, at the major outer and inner surface barriers of the body, and are constantly exposed to agents from the environment. Therefore, these cells probably need to discriminate between infectious and noninfectious agents to avoid unnecessary inflammation. The present study demonstrated that they secrete antibacterial factors only when they receive stimuli from both classical proinflammatory cytokines delivered by innate immunity–type cells and Th17 cytokines delivered by T cells. Thus, an attractive hypothesis is that epithelial cells have been equipped by evolution to respond poorly to the first alert

signal, i.e., the classical proinflammatory cytokines produced by innate immunity cell types, which might be evoked even by noninfectious agents. Infectious agents, such as *S. aureus*, could evoke the production of the second alert signal, i.e., Th17 cytokines produced by T cells, in addition to the first alert signal. This would allow the epithelial cells to respond selectively to pathogens. In HIES patients, the second alert signal is not delivered because of the Th17 deficiency, which probably results in skin- and lung-restricted staphylococcal infections.

Accumulating evidence indicates that Th17 cells and their products are very important in the induction and propagation of autoimmunity (5–10). Therefore, the neutralization of Th17 cytokines appears to be a promising therapeutic strategy for the control of inflammation in autoimmune disorders. Moreover, antagonists of STAT3 are considered good candidates for the treatment of tumors because a variety of tumor cells show up-regulated STAT3 expression (46). However, our data indicate that such treatments would render patients susceptible to staphylococcal infection, particularly of the skin and lung, as observed in HIES. Fortunately, our study also suggests that this undesirable side effect might be prevented or treated by the local application of neutrophil-recruiting chemokines and BDs or their derivatives.

In summary, we demonstrated in the present study that T cells from HIES patients, in spite of their defect in production of Th17 cytokines, showed normal production of other proinflammatory cytokines including IL-1β in response to staphylococcal antigens, which was insufficient for triggering keratinocytes and bronchial epithelial cells but sufficient for other cell types to produce antistaphylococcal factors. This provides a possible molecular explanation for the apparent contradiction between the systemic Th17 deficiency and the skin- and lung-restricted staphylococcal infections in HIES patients.

MATERIALS AND METHODS

Patients. All eight patients enrolled in this study had typical findings associated with HIES and a National Institutes of Health score >40 points (27). The diagnosis was confirmed by the identification of the mutations in the *STAT3* gene. The study was approved by the Tokyo Medical and Dental University Ethics Committee, and written informed consent was obtained from the patients. All of the patients were in a healthy state when their blood samples were collected. Blood samples from patients and age-matched healthy subjects were obtained and PBMCs were prepared by density-gradient centrifugation.

Cell culture. PBMCs were cultured in 96-well plates in RPMI medium 1640 supplemented with 1% penicillin/streptomycin, 1% glutamine, and 10% heat-inactivated FCS. Cultures were stimulated with a 1:100 (vol/vol) dilution of anti-CD3 and anti-CD28 beads (Invitrogen). For some experiments, the following mAbs, cytokines, and TLR ligands were added: 20 ng/ml IL-17A, 200 ng/ml IL-17F, and 200 ng/ml IL-22 (R&D Systems); 10 ng/ml TNF-α, 10 ng/ml IL-1β, 10 ng/ml IFN-γ (PeproTech); neutralizing antibodies against IL-17, IL-22, and BD3 (R&D Systems); TLR ligands (InvivoGen); fixed *S. aureus* (EMD); SEB (Toxin Technology); and *C. albicans* skin test antigen (Torii Pharmaceutical Co., Ltd).

Culture of human keratinocytes, bronchial epithelial cells, fibroblasts, endothelial cells, and macrophages. Human epidermal keratinocytes and bronchial epithelial cells (Lonza) were propagated as adherent cells to plastic in RPMI 1640 medium containing bovine pituitary extract, human epidermal growth factor, insulin, hydrocortisone, gentamicin, and amphotericin at 37°C in a 5% CO_2 incubator. Human primary dermal fibroblasts, HUVEC, HMVEC-L were obtained from Lonza. Macrophages were derived from adherent cells in PBMCs cultured in the presence of 30 ng/ml GM-CSF for 7 d.

RNA isolation and real-time quantitative RT-PCR. Cells were harvested for total RNA isolation using the RNeasy Miniprep kit (QIAGEN), according to the manufacturer's instructions. Total RNA was reverse transcribed using the PrimeScript transcription kit (Takara Bio Inc.). An aliquot of the RT reaction was used as a template for real-time PCR in triplicate using a SYBR Green MasterMix (Takara Bio Inc.) on an Mx3005P thermocycler (Agilent Technologies) with SYBR green I dye as the amplicon detector and ROX as the passive reference. The gene for HPRT was amplified as an endogenous reference. Quantification was determined using both a standard curve and comparative ΔΔCT methods.

ELISA. Conditioned medium from cultured cells was collected after the cells were stimulated and stored at −80°C until use. IL-17A (eBioscience), IL-22 (R&D Systems), IFN-γ, TNF-α, IL-1β, CXCL8 (BD), BD2 (KOMABIOTECH), and BD3 (Alpha Diagnostics) were measured in triplicate by ELISA according to the manufacturers' instructions.

Bactericidal activity against *S. aureus*. *S. aureus* (strain Rosenbach 1884) was obtained from the National Biological Resource Center. Bactericidal activity was evaluated by plating serial dilutions of *S. aureus* mixed with the supernatant from keratinocytes or bronchial epithelial cells, and the CFUs were determined in triplicate on the next day. In some experiments, a neutralizing antibody to BD3 was added to the supernatant.

Chemotaxis. Chemotaxis of neutrophils was determined in triplicate by the Boyden chamber technique. The migration chamber was divided into upper and lower compartments by a membrane with a pore size of 3 μm. The neutrophils were placed into the upper compartment at a concentration of 10^6/ml, and the lower compartment contained the supernatant from the keratinocytes or fibroblasts grown under the conditions indicated. The chambers were incubated at 37° C for 1 h, and the number of neutrophils that migrated to the lower chamber was counted.

Immunoblotting. Cells were lysed on ice for 30 min in lysis buffer containing 1% Triton X-100, 50 mM Tris, pH 8.0, 150 mM NaCl, 2 mM EDTA, 2 μg/ml aprotinin, and 100 μg/ml PMSF. The cell lysates were subjected to SDS-PAGE, followed by electrotransfer to PVDF membranes and immunoblotting with antibodies for IL-1R1, IL-1R2, and IL-1Ra (R&D Systems) and for tubulin (Sigma-Aldrich).

Statistical analysis. Data were compared by a two-tailed Mann-Whitney *U* test or unpaired Student's *t* test. P-values < 0.05 were considered significant.

Online supplemental material. Fig. S1 shows the quantitative RT-PCR analysis for chemokine and BD expression in activated keratinocytes. The importance of IL-17A and IL-22 in stimulating keratinocytes to produce antistaphylococcal factors is demonstrated in Fig. S2. Fig. S3 shows the quantitative RT-PCR analysis for chemokine and BD expression in various types of cells. Production of CXCL8 by keratinocytes and fibroblasts in response to various cytokines is displayed in Figs. S4 and S5. Fig. S6 shows the expression and production of antistaphylococcal factors by keratinocytes in response to various stimuli. Up-regulation of the Th17 cytokine receptors in keratinocytes in response to classical inflammatory cytokines is displayed in Fig. S7. Online supplemental material is available at http://www.jem.org/cgi/content/full/jem.20082767/DC1.

This work is supported by Grants-in-Aid 16616004, 17047013, and 18659299 from the Japanese Ministry of Education, Culture, Sports, Science and Technology and Research on Intractable Diseases from the Ministry of Health, Labor and Welfare, the Uehara Foundation, Naito Foundation, and the Mother and Child Health Foundation.

The authors have no conflicting financial interests.